Lappeenranta University of Technology
School of Engineering Science
Degree Program in Computational Engineering and Physics (Technical-Physics)

Ali Saghi

Highly Perceivable Tactile Feedback by Magnetic Shape Memory (MSM) Technology

Examiners: Dr. Kari Ullakko
Researcher Andrey Saren

Supervisors: Dr. Kari Ullakko
Researcher Andrey Saren

ABSTRACT

Lappeenranta University of Technology
School of Engineering Science
Degree Program in Computational Engineering and Physics (Technical Physics)

Ali Saghi

Highly Perceivable Tactile Feedback by Magnetic Shape Memory (MSM) Technology

Master's Thesis

69 pages, 48 figures, 9 tables

Examiners: Dr. Kari Ullakko
Researcher Andrey Saren

Keywords: MSM actuator, haptic sense, haptic surface, touch surface, HCI

This study concentrates on providing haptic feedbacks on an Aluminum surface using a push-push design MSM actuators. These actuators are created based on the idea of MSM effect which was invented by Kari Ullakko in 1996 at MIT. During last 30 years HCI has experienced a very significant development not only in vision interfaces but also in Haptic interfaces. Most of haptic devices use piezoelectric actuators that are very expensive. The goal of this project is to introduce MSM actuators as a comparable alternative actuator in many aspects including price, mechanical time, power dissipation and so on. Our results show that participants are able to perceive three of Haptic feedbacks with 100%, one ~95% and one in ~85% which is quite considerable. Therefore, we believe that MSM actuators can be the next industrial actuators in the world of haptic interfaces.

Acknowledgment

This research work is performed at LUT Material Physics Laboratory, located in Savonlinna, in collaboration with Tampere Unit for Computer-Human Interaction (TAUCHI) at university of Tampere.

Once a project is done, it is very joyful to look at the past and remember all the people who have helped and supported to accomplish this thesis.

- Firstly, I would like to thank in advance to my first supervisor, Dr. Kari Ullakko the head of the Savonlinna laboratory. Kari invented the MSM effect on 1996 in MIT and has continued it until now as o pioneer. For me it was a magnificent opportunity to work under supervision of a scientist. He behaved very friendly and helpful during my work on this project.
- Secondly, I sincerely thank to my Professor Erkki Lähdranta. When I came to Finland in 2015 for my first time, he was our head in physics department and treated us very kindly. Prof. Lähderanta introduced me to Kari and I have to show my deep respect to him.
- The people in Savonlinna Laboratory during 6 months helped me a lot. PhD. Andrey Saren as my second supervisor guided me through this project very well. In addition, I would like to thank to Denys Musiienko who helped me through programing. Special thanks to Janne who made the prototype. Other members of laboratory including Sozinov and Soroka helped the project too friendly.
- Last but not least I offer my special gratitude to Prof. Raisamo, Prof. Hippula and PhD. Nukarinen for their nice hospitality in TAUCHI in Tampere University while we tested the haptic feedbacks.

Contents

1 INTRODUCTION 3

1.1 BACKGROUND 3

1.2 GOALS AND DELIMITATIONS 4

1.3 STRUCTURE OF THE THESIS 5

2 THESIS 6

2.1 MSM EFFECT AND ITS APPLICATIONS 6

2.1.1 Background 6
2.1.2 Shape memory alloys 6
2.1.3 Magnetic shape memory alloys 10
2.1.4 Fundamentals of Ni-Mn-Ga 14
2.1.5 Crystallographic structure 14

2.2 HAPTIC FEEDBACK IN TOUCH INTERACTION 17

2.2.1 Background 17
2.2.2 Vibro tactile feedback parameters 19
2.2.3 Various tactile display devices 23

3 RESULTS 46

3.1 MSM EFFECT-BASED ACTUATOR 46

3.1.1 MSM actuator design 46
3.1.2 Actuation characterization 47

3.2 MSM EFFECT BASED HAPTIC DEVICE (DEVICE AND PROPERTIES) 50

3.2.1 Physical structure of push-push MSM actuator system 50
3.2.2 System parameters 51
3.2.3 Testing of device's haptic feedbacks 53

4 DISCUSSION AND CONCLUSIONS 60

5 SUMMARY 61

REFERENCES 62

LIST OF SYMBOLS AND ABBREVIATIONS

ATM	Automatic Teller Machine
DAC	Digital Analog Convertor
EAP	Electroactive Polymer
ERM	Eccentric Rotating Mass
FMSM	Ferromagnetic Shape Memory
HCI	Human Computer Interface
JND	Just Noticeable Difference
LATPaD	Large Area Tactile Pattern Display
LRA	Linear Resonant Actuator
M	Magnetization
MFIS	Magnetic Field-induced Strain
MIR	Magnetically Induced Reorientation
MSM	Magnetic Shape Memory
MR	Magnetorheological
NI	National Instrument
Ni-Mn-Ga	Nickle-Manganese-Gallium
NM	Non-modulated
PDA	Personal Digital Assistant
RA	Rapid Adaption
SAW	Surface Acoustic Wave
SA	Slow Adaption
SMA	Shape Memory Alloy
TPaD	Tactile Pattern Display
5M	Modulated Five-layered
7M	Modulated Seven-layered

1 INTRODUCTION

1.1 Background

In the previous decade Haptic technology has gotten a big role in commercial applications such as virtual reality, mobile devices, personal computers, video games, simulators and tactile electronic displays. Also there is a huge investigations on the fields like medicine, robotics, arts and holographic. This emerges from the fact that haptic recreates the sense of touch by applying forces and vibrations to the user. Nowadays there is a huge demand for realistic communication with Human Computer Interface (HCI) and researchers have a significant hope on haptic interfaces to become more and more imperative alongside the HCI evolution in such a way that become commonplace as today's visual and audio interfaces.

There are two general category of haptic interfaces. The first category is force feedback devices which use physically push/pull user's body and mostly are applied to game interfaces, medical and training simulators. The other one is tactile feedback applications such as smart phones, tablet PCs, electric readers, public kiosks, ticket machines and Automatic Teller Machines (ATMs) which all have a haptic-surface. The term haptic-surface here means any device which can create a virtual effect on a physical surface that is perceived by human fingertip. However it is clear that the success of these interfaces will only be achieved through the development of a fast, small, strong, silent and safe tactile display interface with a low heat dissipation and power consumption.

Haptic surfaces in a general view are divided to 3 categories as shape changing surface, variable friction and vibrotactile feedback. Shape changing surface is the one category of haptic surfaces in which one can perceive virtual effects by changing the shape of physical surface. Yang et al. [1] presented a 6x5 pin-array that is actuated by 30 piezoelectric bimorphs which can produce micro shapes and vibrotactile feedback on fingertips. Pasquero and Hayward [2] introduced a tactile display system composed of 10x10 laterally moving skin actuated contactors. Velazquez et al. [3] presented an 8x8 tactile pin-array actuated by Shape Memory Alloys (SMAs). It can produce 2.6 mm spatial resolution and 1 mm vertical excursion. By changing the friction between fingertip and physical surface one can produce life-like gestures like move a file, scroll a menu or draw a picture. Levesque et al. [4] introduced Large Area Tactile Pattern Display (LATPaD) using squeeze air film

effect to reduce the friction coefficient of haptic surface from 1.0 to 0.15 by 26 kHz piezo-actuated vibrations. Kotani et al. [5] reduced friction coefficient between surface and fingertip using ultrasonic Surface Acoustic Wave (SAW) by placing piezoelectric actuators at the edges of the device. Bau et al. [6] increased the friction coefficient through increasing of normal force using electrovibration principle in TeslaTouch. Dai et al. [7] developed the Lateral Pad which can produce lateral (shear) force around 70 mN on a bare finger.

A very typical example of this category is the phone alarm vibration generated by a vibration motor in mobile phone. Therefor an actuator can be located beneath the touch surface, attached to the body of device or placed inside the interface. Currently there are two types of inertia actuators as Eccentric Rotating Mass (ERM) and Linear Resonant Actuator (LRA). ERM can generate vibration easily but the vibrotactile feedback is not sharp since its low respond speed and latency. LRA can generate sharp and crispy vibrations but its limitation is low frequency bandwidth just around resonance frequency [8]. Yatani and Truong [9] presented SemFeel in which 5 vibration motors are attached to the backside of a mobile touch screen device. User can differentiate 3 patterns as: Positional, Linear and Circular patterns. Comparing to ERM, voice coil has a smaller latency. Fukumoto [10] proposed a button-click feedback by embedding a voice coil in a mobile phone. Brewster et al. [11] introduced the Tactons which generate different vibrotactile feedback using a range of parameters such as frequency, amplitude, duration, rhythm and location. Solenoid is actuated by magnetic force like voice coil and unlike inertia actuators can be controlled by modulating frequency and amplitude [12]. PiPoupyrev et al. [13] embedded four piezoelectric actuators named as TouchEngine [14] in the corners of a Samsung PDA between the display and touch sensitive glass. They generated different gestures such as click buttons, scroll bars and menus where the vibration was localized.

1.2 Goals and delimitations

Considering all actuator technologies such as servomotors, electromagnetic coils, piezoelectrics, shape memory alloys and fluid and their advantages and disadvantages, it seems none of these above mentioned technologies are able to satisfy the great need of current technology for vibrotactile displays. In one hand, piezoelectric and

magnetorestrictive materials demonstrate rapid response but their strokes are small. In the other hand, SMAs have a large stroke but their thermomechanical control is slow.

The world of mechanical engineering needs actuators that exhibit a large stroke under precise and rapid control exhibit. In 1996 Kari Ullakko proposed the idea of Magnetic Shape Memory (MSM) effect [15] that magnetically control these smart materials. By applying a magnetic field on these materials the reorientation of the twin structure of martensite happens and leads to actuation. Since these materials provide large enough strokes in a rapid and precise control, can be considered as new types of vibrotactile actuators.

In this project we introduce a new smart material based actuator as MSM alloy actuator. By creating a maximum 100 Hz and around 1 mm displacement on an Aluminum surface which is touched by a bared fingertip plus apply other parameters like duration and rhythm, one can highly perceive and differentiate between various vibrotactile patterns.

1.3 Structure of the thesis

In section 1 I explained a short history of MSM effect, the way it creates actuation and some applications of these actuators in the industry plus a list of advantageous and disadvantageous of MSM technology. Section 2 is discussing about sensitivity of skin, vibrotactile haptic parameters and various vibrotactile applications that were created during past decade. Characterization of our MSM actuator is discussed in section 3. Last but not least in the result section our prototype design and experiment that we did are provided.

2 THESIS

2.1 MSM effect and its applications

2.1.1 Background

SMAs are alloys which “remember” their original shapes and that when deformed, return to their pre-deformed shape. Therefore they are called “smart materials”. They can come back to their origin shape from a large permanent deformation and also from a large strains by slightly increase the temperature and by applying loading and unloading, respectively. The mechanism responsible for such a phenomenon is martensite transition from an open symmetry phase to a close-packed structure. Nowadays in the market these materials are so considerable due to their applications in sensors and actuators. Slow mechanical response to temperature changes which leads to a notable loss of potential energy, is a disadvantages of thermally controlled SMA actuators. To overcome of this problem, MSM alloys are promising to decrease the response time by using magnetic controlled shape memory effect.

2.1.2 Shape memory alloys

Thermo-elastic martensitic transformation of the crystal lattice is the most essential property of a material which belongs to SMAs. In martensitic transformation in Fig. 1, the crystal structure changes from parent martensite which has a tetragonal or orthorhombic crystal structure to a high symmetry cubic austenite phase. Also in Fig. 2 the twin boundaries that separate different twin variants, are shown.

Slipping plastically of martensitic planes may leads to an ensemble of twin variants which is separated by mobile twin boundaries. Comparing the motion of the twin boundaries and slipping, the first one is the easiest way to deform the sample since it involves breaking fewer chemical bounds in the lattice and also it explains the microscopic shape change very clear [16].

As it is obvious in Fig. 3, the transformation starts at temperature As and finishes at Af. In the reverse transformation the start temperature is Ms and the final is Mf. Since this transformation is hysteretic, it implies that the reverse process occurs at different temperatures comparing to the original one.

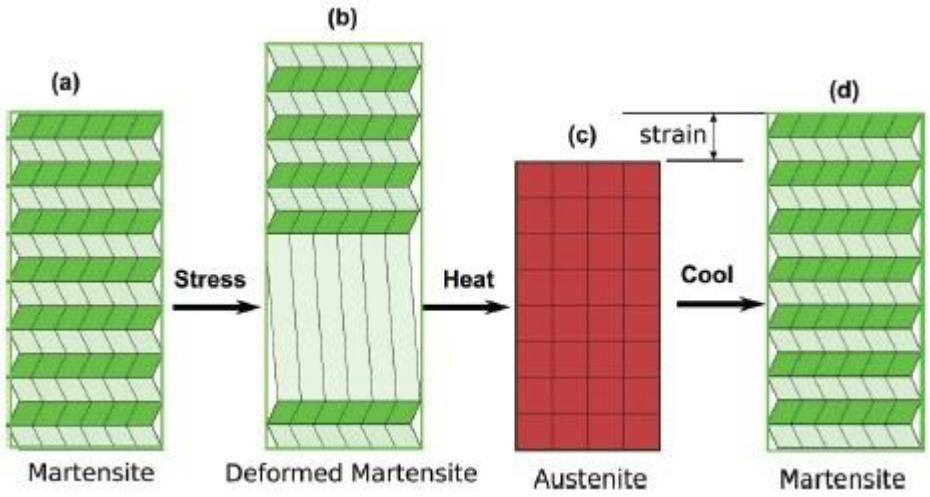

Fig. 1. Martensite transformation. (a) The parent martensite phase, (b) deformation of material by an external stress, (c) heating the sample to high temperature to induce austenite phase, (d) original shape is restored upon cooling the sample from the high temperature austenite. [16]

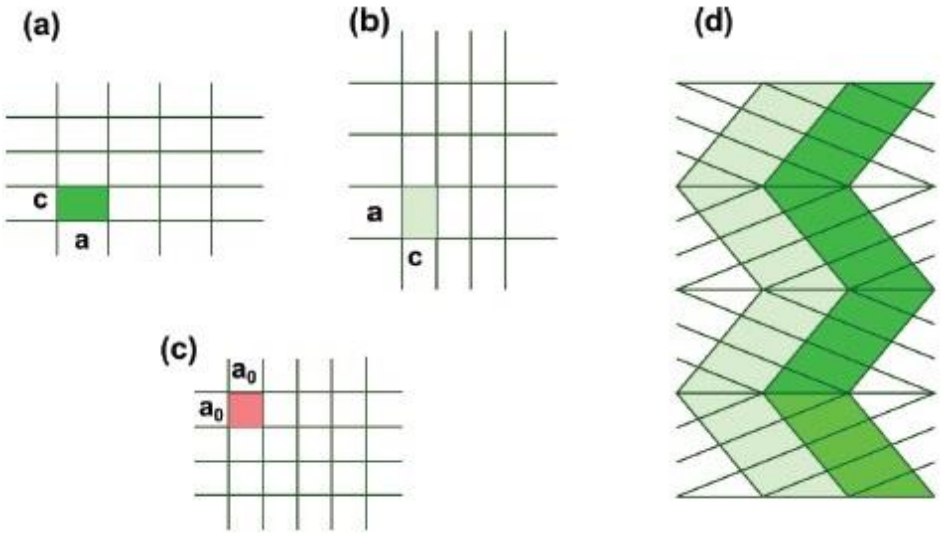

Fig. 2. Formation of twin boundaries in two dimensions in NiTi. (a), (b) Two different martensitic variants crystal structure, (c) final austenite phase for cubic structure, (d) martensitic variants separated by twin boundaries. [16]

The amount of elastic and surface energies, which are stored during transformation control the width of this hysteresis. Consequently the narrower the width of the loop the easier it is to transform from one state to the other one by heating and cooling. Maximum thermal hysteresis of some alloys is in the order of 50ºC or even more but the common temperature order is around 10-20ºC [17].

According Fig. 4, in one-way procedure when the material is in its martensite state, it

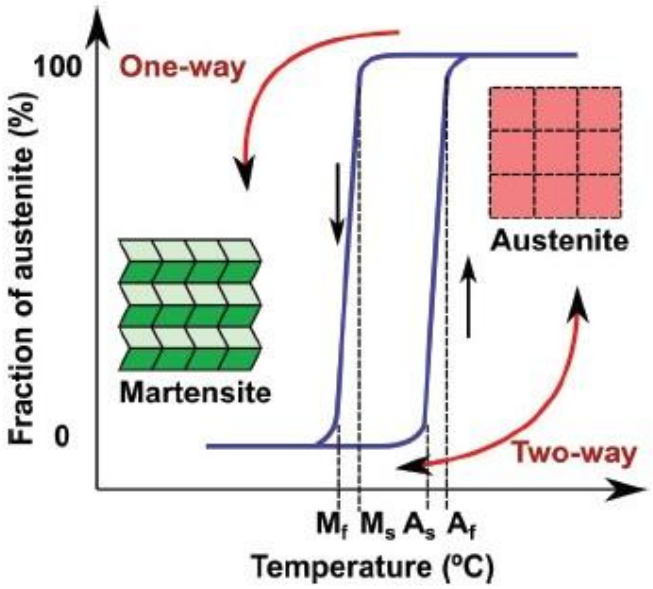

Fig. 3. Temperature hysteresis using shape memory effect where low temperature is martensite phase and high temperature is austenite phase. [16]

can be bent or stretched but will hold this shape until heat enough to reach the transition temperature. When the sample cools again nothing will happen and it remains in the austenite phase until it deformed again. We can say in one-way effect material remembers the shape of martensite state [18].

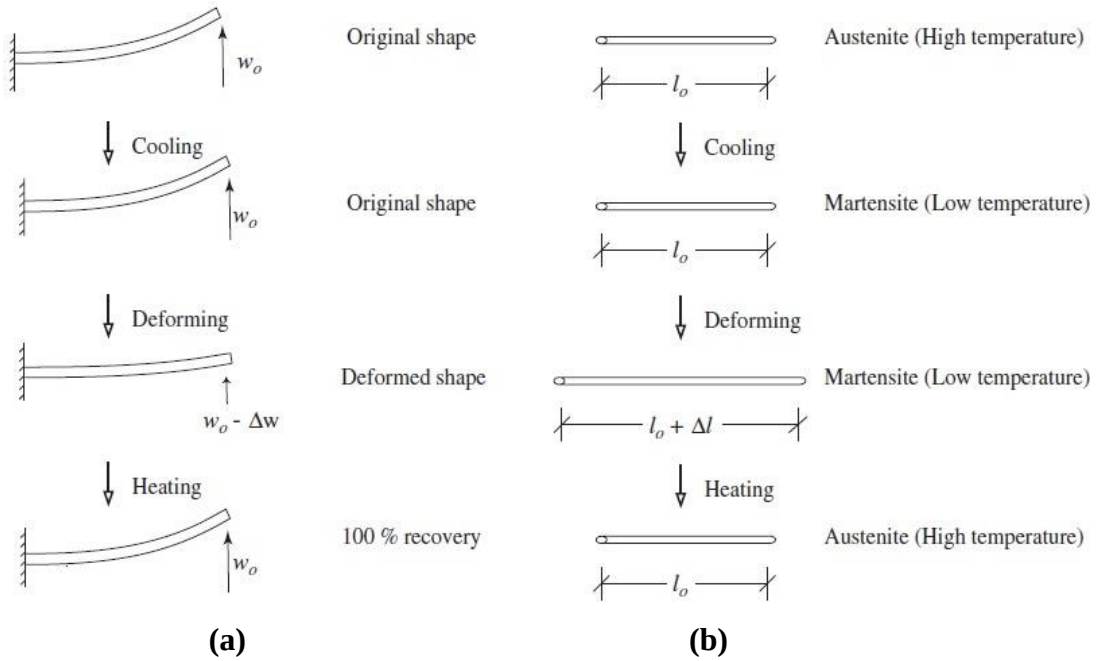

Fig. 4. Two types of one-way shape memory effect. (a) Beam bending, (b) Beam extension. [18]

In the other hand as Fig. 5 shows, two-way effect is one in which the material can remember two shapes, one in austenite phase and the other in martensite.

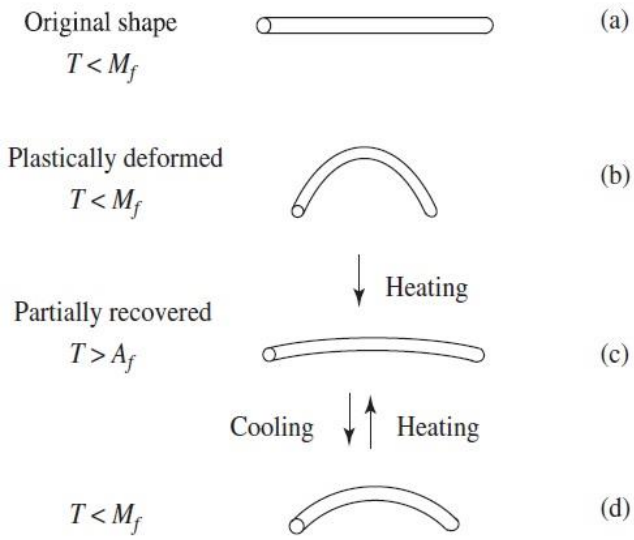

Fig. 5. Two-way shape memory effect. (a) Martensite phase, (b) partially deformed, (c) partially recovered, (d) austenite phase. [18]

One-way shape memory effect was discovered in 1951 in a Gold alloy that had around 47.5% Cadmium. After finding this phenomenon in NiTi, this effect became very famous in industry [19].

As it is shown in Fig. 6, in superelasticity phenomena the temperature can be fixed during all process. Therefore transforming from austenite to martensite phase will happen not in response to changing the temperature but in response to loading a mechanical stress. By increasing the stress gradually, the sample will transform from an unstressed austenite phase to the martensite state above critical stress that is proportional to temperature transformation. By continuing loading, twinned martensite will change to detwinned martensite. This allows the material to bear large strain. When the mechanical stress is released, the material will return to austenite phase and will recover its original shape means again it will be twinned austenite. Some these materials can reversibly deform to high strains such as 8% [20].

In shape memory effect, Fig. 6, at first the material is in twinned martensite phase. By loading the mechanical stress it will transform to stressed detwinned martensite above critical stress. Now if we decrease the load it will came back to unstressed detwinned martensite. By heating, the material will go to unstressed austenite and from there by

cooling will return to the first phase.

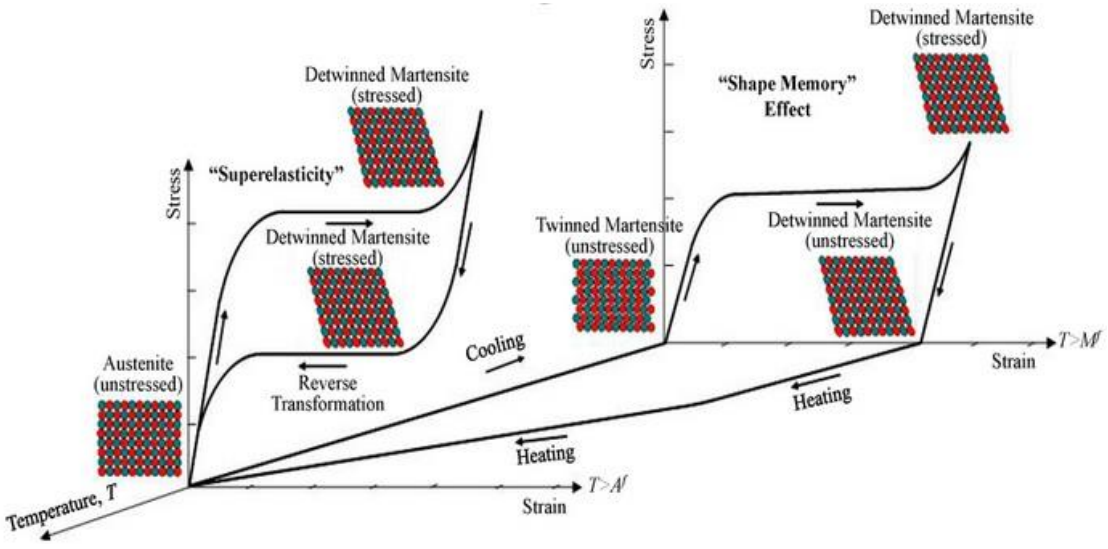

Fig. 6. Comparing "Superelasticity" and "Shape memory effect" in respect to Stress, Strain and Temperature.

2.1.3 Magnetic shape memory alloys

MSM alloys or FMSM alloys are specific type of shape memory alloys that can produce force and stroke under a magnetic field. In addition, these materials are able to produce force and deformation in response to temperature. Usually MSM alloys are alloys of Nickel, Manganese and Gallium (Ni-Mn-Ga).

Kari Ullakko and his co-workers at MIT discovered a magnetically induced strain around 0.2% in stoichiometric Ni50Mn25Ga25 specimen under 0.8T magnetic field and they interpreted that this effect is because of rearrangement of martensite structure [15]. After the first demonstration, there have been many improvements to increase the magnetic induced-actuation and the result is from 0.2% to 0.6%, which is close to the theoretical maximum strain of a tetragonal crystal structure [21]. In 2002, Sozinov et al. observed the magnetic field induced deformation of 10% in Ni-Mn-Ga [22].

People also observed the magnetic field induced deformation in Ni-Mn-Ga-Fe, Fe-Pd, La-Sr-CuO4, Fe-Ni-Co-Ti, Fe-Pt, Co-Ni-Ga, Ni-Mn-Al and Co-Ni-Al alloys [16]. Although there are many magnetic shape memory alloys but since the $Ni2$Mn-Ga heusler alloys have unique magneto-mechanical properties, practically these materials are under investigations [23].

Since the MSMAs have considerable magnetically induced deformation and a very short response time, which is comparable with piezoelectrics, they are very attractive to be used in actuators and being applied in the fields such as pneumatics, robotics, medical devices and mechatronics [24]. Furthermore they can be used as displacement, speed and force sensors and mechanical harvesters since along actuation, they can change their magnetic property depend on deformations [25].

Magnetically Induced Reorientation (MIR) is the reason behind large strain in MSM alloys, which is illustrated in Fig. 7. The mechanism can be explained in a way that like other ferromagnetic alloys when MSM alloy is subjected to an external magnetic field, elementary magnetizations gradually get aligned with the magnetic field direction and therefore MSM will exhibit a macroscopic magnetization.

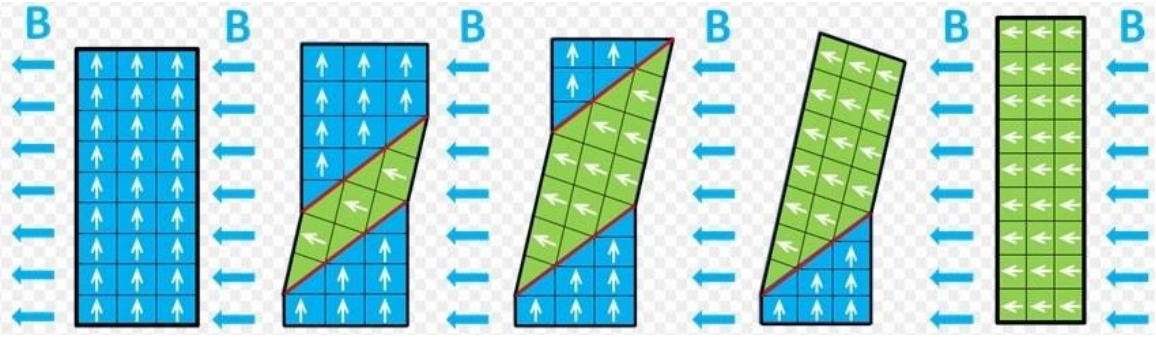

Fig. 7. Magnetic shape memory working principle. Note that the deformation kink shown in the figure is just for illustration but in reality, the kink is < 4°. [26]

There is just one difference since in the MSM alloy, the alignment is occurred by the geometric rotation of the elementary cells composing the alloy but in a typical ferromagnetic material, the alignment is obtained by rotation of magnetization vectors inside the cells that in Fig. 8 is obvious.

When a MSM alloy is subjected to an external force, macroscopically the similar phenomenon will happen and the cells composing the alloy will rotate geometrically. In contrast to elongation that is produced under magnetic field in Fig. 7, in Fig. 9 it is shown that by applying an external force to a sample contraction happens.

Fig. 10 demonstrates the crystallographic structure of Ni2Mn-Ga in high temperature austenite that is cubic and in low temperature martensite that shows a tetragonal symmetry.

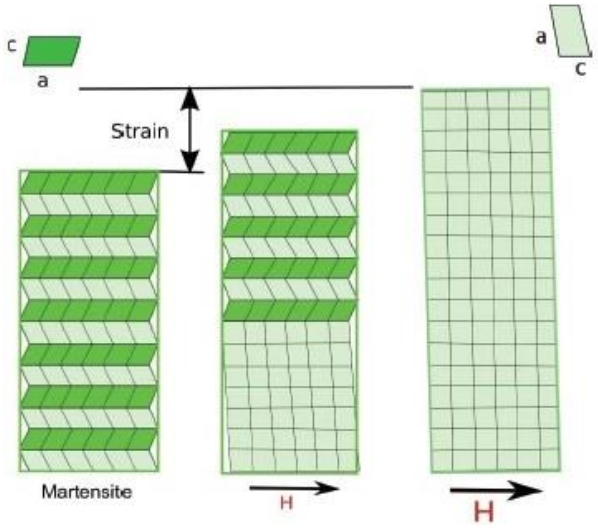

Fig .8. Left: A FSMA sample composing of martensitic variants structure at zero field. Center: When a magnetic field orthogonal to the orientation of variant is applied, a new martesitic variant (light green) parallel to field is produced. Right: Totally elongated shape. [16]

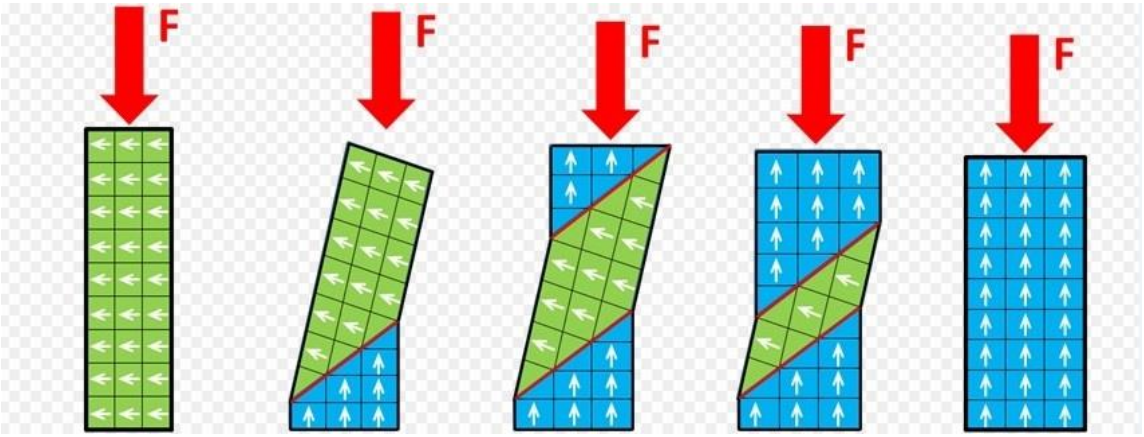

Fig .9. Magnetic shape memory working principle. Note that the deformation kink shown in the figure is just for illustration but in reality, the kink is < 4°. [26]

In martensite phase three different variants are possible which are located along different crystallographic orientations with saturation magnetization direction. These directions are called magnetic easy axis that in this case is aligned with the short edge C of the tetragonal unit cell. The other important point is that the Magnetization (M) can be oriented in positive or negative easy axis direction. Having this configuration if an external magnetic field is applied, one variant will be selected in favor of others according the magnetization

and the magnetic field inside the material. This process is called MIR which was explained above.

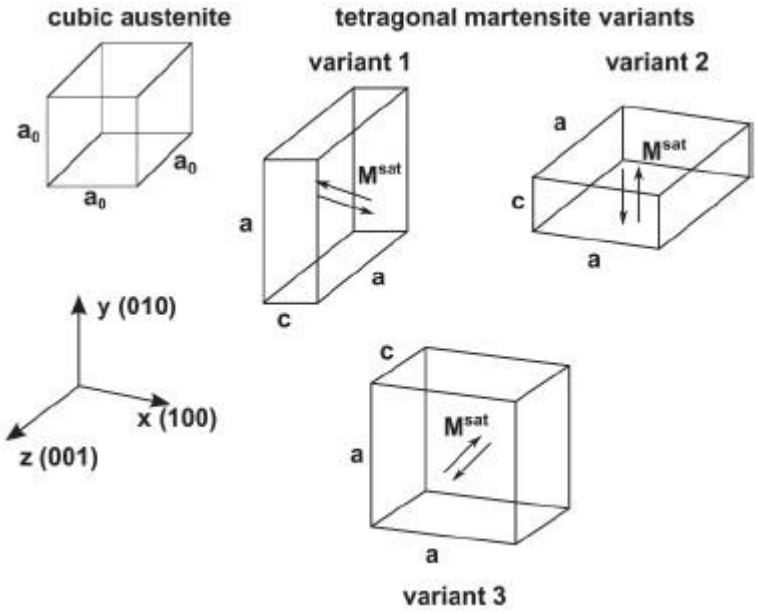

Fig .10. Crystal structure of cubic austenite phase and three different tetragonal martensite variants in Ni2MnGa. [16]

The rotation of the cells inside MSM element is a result of two reasons. The first one is large magnetic anisotropy of MSM alloy and the second one is high mobility of internal regions. The internal regions that are shown by green and blue colors in Fig. 7 and Fig. 9, each have their orientation of the elementary cells and are called twin-variants. The boundaries between these regions are called twin-boundaries that can be shifted by both external magnetic field and force in favor of one region and leads to elongation and contraction. When the material is completely elongated or contracted, just one of these twin-regions forms it and consequently it is in a single variant state. Magnetization's of a MSM alloy is different if the sample is in contraction or elongation single variant state. The different required energy to magnetize the element in contraction single variant state and in elongation single variant state is called magnetic anisotropy. This magnetic anisotropy is related to the sample's maximum work-output and consequently related to strain and force that is applied in applications [27].

2.1.4 Fundamentals of Ni-Mn-Ga

It was reported that it is possible to create ferromagnetic alloys from non-ferromagnetic samples for instance Cu2MnAl by Friedrich Heusler in 1903. These X2YZ Heusler alloys have received huge attention because of their ferromagnetic property and the magnetic shape memory effect that is related to temperature driven martensite transformation. In 1960, Hames et al studied the ferromagnetic properties of the Heusler alloy Ni2MnGa and in 1962 Martynov and Kokorin were studied the effect of temperature on the alloy's crystal structure. In 1995 as mentioned before, Ullakko invented the magnetic shape memory effect and demonstrated a reversible Magnetic Field-induced Strain (MFIS) of 0.2% in a NI-Mn-Ga alloy at 265 K [28].

2.1.5 Crystallographic structure

The high temperature of austenite phase of Ni-Mn-Ga follows the highly ordered FCC L21cubic structure that is characteristics of Heusler alloys. In figure 2.13 the atomic positions of nickel, manganese and gallium atoms of stoichiometric Ni2MnGa is shown in the austenite phase [28].

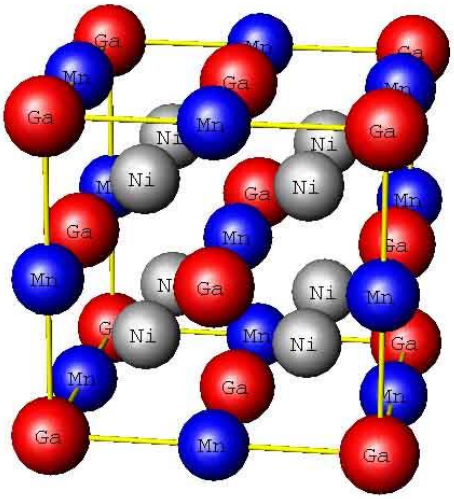

Fig. 11. The FCC L21cubic structure of stoichiometric Ni2MnGa in its austenite phase. Gallium atoms are red, manganese atoms are blue and nickel atoms are grey. [29]

According to the Fig. 11, gallium atoms (red) are located in each corner and in the center of each face of the unit cell. Manganese atoms (blue) are located between gallium atoms at

the center of each edges and as well as the center of the unit cell. The nickel atoms (grey) are located at the center of each of eight sub-unit cells.

As the material is cooled, it distorts and transforms from a high symmetry austenite lattice into a low symmetry martensite crystal structure. The structure of martensitic Ni-Mn-Ga is extremely affected by some parameters such as composition of the alloy, temperature and applied stress to the material.

According to PhD thesis of Aaron R.Smith "The Ni-Mn-Ga can be characterized using properties as follow:

- The ratio of the c-axis and the a-axis of the martensitic unit cell. This ratio defines the theoretical maximum strain that is possible by reorientation of the crystal lattice using the equation ε=1-c/a.
- The twinning stress σtw that defines minimum stress and thus the minimum magnetic field which is needed to deform the material.
- The blocking stress, σmag, which defines the maximum stress using magnetic field.
- As the austenite transformation strain temperature that defines the maximum temperature in which the material will remain in martensite phase."[28].

Tetragonal structure of the Non-modulated (NM) Ni-Mn-Ga and its twinning stress which is much greater than its blocking stress leads to a non-considerable strain thus is not studied enough. In the other hand both modulated seven-layered (7M) and modulated five-layered (5M) Ni-Mn-Ga are extensively studied. 7M Ni-Mn-Ga has a pseudo-orthorhombic structure with a **c/a** ratio of 0.90 and a **MFIS** of 9.5%. Both parameters seem great except its structure that is considered metastable and the blocking stress of 1.6 MPa. Modulated five-layered (5M) Ni-Mn-Ga has the structure of pseudo-tetragonal with a **c/a** ratio of 0.94. Murray et al. showed that its **MFIS** is around 6% which is close to the theoretical maximum possible. People tried to reduce the twinning stress in NM Ni-Mn-Ga such as Likhache et al. who reported twinning stress in 5M Ni-Mn-Ga greater than 1.0 MPa in 2003 and Rolfs et al. who obtained 0.5 MPa in 2009 by minimizing crystal inhomogeneity and impurities. Since 5M Ni-Mn-Ga has the lowest twining stress which is coupled with a high blocking stress of 3.0 MPa and an As above room temperature, therefore it will be on the point of focus. Crystallographic details of Ni-Mn-Ga in its

austenite and different martensite structures are reported in Table 1 [28].

Table 1. The crystal structures and lattice parameters of Ni-Mn-Ga in its austenite phase and various martensite phases. [28]

Material Phase	Crystal Structure	Crystallographic Space Group	Lattice Parameter (Å)		
			a	b	c
Austenite	Cubic	Fm-3m	5.82	5.82	5.82
7M Martensite	Pseudo-Orthorhombic	Fmmm	6.12	5.80	5.50
5M Martensite	Pseudo-Tetragonal	L4/mmm	5.94	5.94	5.59
NM Martensite	Tetragonal	L4/mmm	5.46	5.46	6.58

2.2 Haptic feedback in touch interaction

2.2.1 Background

The skin is the largest organ in the human body. In the body of an average adult the skin's area is approximately 1.8 m2. A large part of the somatosensory system of the human' body is based on some special ending nerves which are located in different layers of the skin. Using these endings the somatosensory system can produce various sensations in reaction to stimulation upon the skin such as tactile sensation (position of the object on body surface), temperature (stimuli that are warmer or colder than body surface), proprioception (position of the body and limbs in the space) and nociception (stimuli which create pain on the skin).

Here we will focus on tactile sensations since it is related to our work. As in Fig. 12, four mechanoreceptors and free nerve endings will carry the sensation to the human's skin. Like mechanoreceptors, free nerve endings can feel touch, pressure, stretch and temperature but their first priority is feeling pain therefore we will focus on these four mechanoreceptors including: Merkel's disks, Ruffini endings, Meissner corpuscles and Pacinian corpuscles.

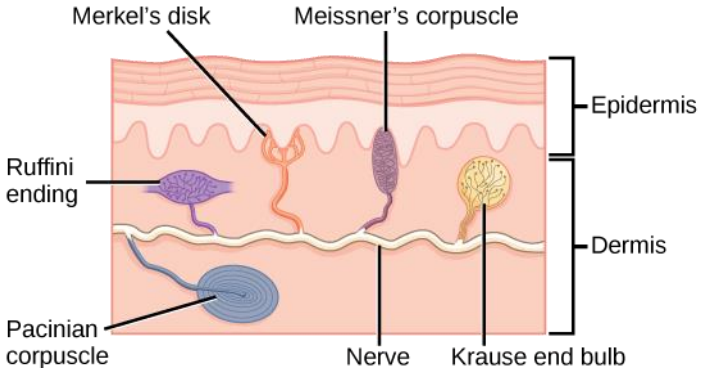

Fig. 12. Cross section of the skin. Four mechanoreceptors alongside the free nerve endings which are located in two layers, dermis and epidermis, are responsible for sensing the tactile sensations. [30]

According to the studies till now, there is not a specific tactile sensation as the reaction of one specific activated mechanoreceptors but all mechanoreceptors will be affected and will react to the stimuli at the same time. However as it is shown in the Table 2, every

mechanoreceptors has its sensitivity bandwidths in frequency that is related to its specific perception. Therefore frequencies below 1 Hz will create pressure on the body surface when frequency more than 50 Hz will affect the skin by vibratio.

Table 2. Characteristics of the four mechanoreceptors. SA (Slowly-adapting), RA (Rapidly-adapting)

	Merkel disk	**Ruffini ending**	**Meissner corpuscle**	**Pacinian corpuscle**
Property	SA Type I	SA Type II	RA Type I	RA Type II
Sensation	Pressure	Stretch	Tap, Flutter	Vibration
Frequency	0.4-1, 5-15	150-400	25-40	200-300
Field area	Small(12.6)	Large(101.0)	Small(11.0)	Large(59.0)
Adaption	Slow	Slow	Rapid	Rapid

Row number three is the field area in which the mechanoreceptor is able to percept the tactile sensation of the stimuli. In Fig. 13 mechanoreceptors and their affected areas are shown. The smallest area belongs to Meissner's corpuscles and the largest one belongs to Ruffini endings.

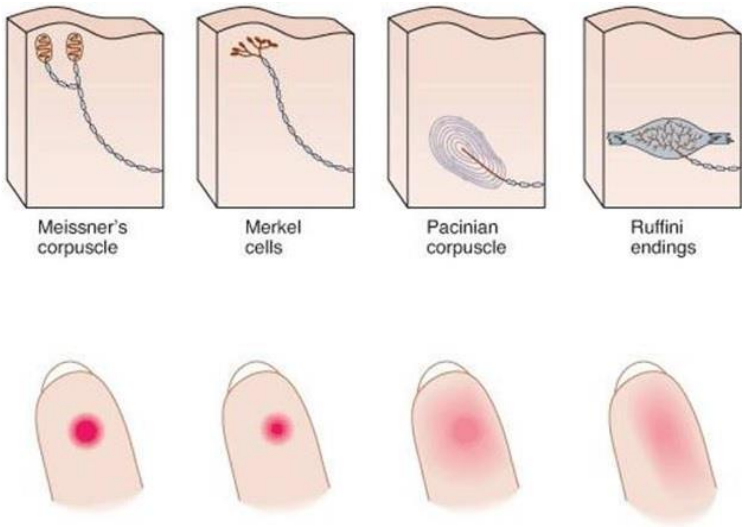

Fig. 13. Four mechanoreceptors and their fields of areas on the fingertips. [31]

In the first and last rows of Table 2, these mechanoreceptors are compared or characterized according to their rate of adaptations. When a mechanoreceptor receives a stimulation, it starts to fire impulses in nerve system but after a while this stimuli will subside in the nerve system and consequently the receptor will adapt to a static stimulus. This process is

called adaption which has two types, Slow Adaptation (SA) and Rapid Adaptation (RA). Meissner's corpuscle and Pacinian corpuscle are in the rapid adaption rate (after receiving the initial stimulus, impulses in the nerve system becomes weak rapidly). These two above mentioned mechanoreceptors are helping to the rapidly changing stimulation such as texture and vibration.

Since our haptic application uses vibration sensation thus it is good to note carefully on the Pacinian corpuscle which is responsible for creation of vibration on the skin. According to the Fig. 12, a Pacinian corpuscle is an oval-shaped mechanoreceptor that its length and width are respectively 1.0 mm and 0.5 mm. The reason for being very sensitive to vibration is 50 or more concentric layers of tissue which are located around sensory nerve. The frequency bandwidth of these receptors is between 200 Hz and 300 Hz thus the best frequency will be 250 Hz a spatial vibration of approximately 200 μm. In the figure below these two parameters (frequency and vibration displacement) are compared.

2.2.2 Vibro tactile feedback parameters

Intensity

Intensity which in most cases is called amplitude, means the strength of viberation and normally is very easy controllable therefore it is the most famous parameter among others.

In 1960 Geldard demonstrate that every part of human body's skin has its susceptibility to discomfort and damages when face with powerful vibrations. He showed that in the chest area 50-400 μm can be considered as the range of stimulus amplitude. A person can perceive the lower limit stimuli, 50 μm, with 100% accuracy. 400 μm is the upper limit where a person perceives the stimuli without any discomfort or pain resulted by strong vibration. Later in 1992 Verrillo & Gescheider discovered that the upper limit in which a person would not have any discomfort perceiving the vibration intensity is 55 dB [32].

Geldard also showed in the same study that 15 different levels of intensity are noticeable in the above mentioned range. Two studies also showed Just Noticeable Differences (JNDs) (smallest noticeable difference between initial and current level of stimuli) for some sensation levels. Firstly, in 1972 Craig reported a JND close to 2 dB when the viberation level is 20 dB. Then in 1988 Bolanowski Jr. et al. demonstrated that JND can be around 0.7-2.5 dB when the sensation level is 4-40 dB. According these results, it is obvious that indicating a precise value for JND is very difficult since JNDs depend on the stimulus

intensity but it seems a JND in the range of 1-3 dB is a good approximation [32].
As it was mentioned above in theory the different noticeable levels of intensity are 15 but in realistic situation as Geldard reported, distinguishing more than 3 would be hard. Also in 2002 Van Erp suggested that the number of different level of intensities should not more than 3 otherwise it would not be distinguishable [32].
Brown et al. in 2006 studied the accuracy of human body to detect different intensity changes. They found that human body can recognize three different intensity changes with accuracy around 92-100% [32].

Duration

Duration of the stimuli on the human body is the other parameter of vibrotactile feedbacks which means the temporal length of vibration. AS Geldard suggested, in the range of 0.1 to 2.0 sec participants can have 25 JNDs in a way that 50 msec difference at the low limit and 150 msec for the higher one [32].
In another study Gescheider in 1966 investigated the ability of human body for perceiving the duration of two stimuli on different parts of the fingers. For this reason, he proposed three experiments. In the first trial participant would experience two stimuli on one index fingertip. Secondly he put one stimuli on the index fingertip and the other stimuli on the ring fingertip both in one hand. And last but not least one stimuli on each index fingertips. He found that if the second stimuli could stronger than the first one by 5 dB, people could recognize the difference timing activation of two stimuluses by minimum time difference of 10.0-12.5 mesc [32].
Considering these results, it seems the parameter duration has a high resolution output but keep in mind that all these results are obtained when other external factors are removed otherwise in a realistic situation one can easily miss or mis-recognize the short vibrotactiles.

Frequency

In the field of haptics frequency means the number of vibration cycles during in one sec therefore the unit will be in Hz. In 1999 Goldstein proposed that the mechanoreceptors in human skin have the ability to respond the frequencies from 0.3 Hz to 500 Hz. However according to table 3.1 not all the frequencies in this range can be sensed and therefore are

not suitable for practical applications. To finding the best frequency range for perceiving vibration, people such as Gescheider and Verrillo in 2002 investigated and the result was 150-300 Hz. This range is called optimal since it requires the lowest threshold amplitudes to be perceived otherwise the rest of the frequency range can be felt but it requires much higher amplitudes to be sensed [32].

In 1928 Knudsen investigated on index fingertip and proposed that for the frequency range of 64-512 Hz when the stimulus level is 34 dB, the average JNDs ratio was 15-30%. The same investigation was conducted by Gebhard in 1957 and showed that the average JNDs ratio was 2-8% when the frequency range was between 1 Hz and 320Hz. In the other experiment, Goff obtained a JND ratio of 18-36% when stimuli were 20 dB and 31-55% with the stimuli of 35 dB. According to these investigations it seems the human skin is not very sensitive to absolute values of vibration frequency [32].

However, Rothenberg et al. in 1977 proposed that people can perceive the small JNDs when the frequency of one stimuli changes over time better than when two stimuli with different frequencies are given. Therefore, one can claim that the skin is more sensitive to change of vibration frequencies than to absolute values of vibration frequencies [32].

Overall we should keep in mind that all these investigations are not standardized till now and the new studies are quite necessary to measure the sensitivity of skin to vibration frequencies.

Waveform

The shape of the input signals to a tactile actuator is called waveform. There are some familiar waveforms including sine, sawtooth and square waves which among them the sine waveforms are widely used to feed the tactile actuators.

Brewster & Brown in 2004 proposed that applying the shape of waveforms in sound design is more accurate than use them in tactile simulation designs. Also Brown in 2007 studied some commercially tactile actuators and showed that the output waveforms were not as the input waveforms except the sine waves. Thus currently available tactile actuators do not reproduce the exact input waveforms. Considering these problems, it is possible to use the idea of modulated sine wave which can be produced by multiplying two sine waves that have different frequencies. In the figure … these different types of waveforms that can be

applied as input of tactile actuators are demonstrated [33].

In 1986 Wisenberger conducted an investigation between modulated sine wave and unmodulated sine wave. The result was that participants identified modulated sine waves as rougher than unmodulated ones. According this result Brown, Brewster & Purchase in 2005 used of roughness as a parameter and create three different levels of roughness as smooth, rough and very rough. Participants were capable to perceive the difference between these three levels approximately 80% [33].

However, in the study of Hoggan & Brewster in 2007, it was shown that participants can perceive the difference between three waveforms of sine, square and sawtooth by 94% whereas they could capable to differentiate three different modulated sine waves approximately 61% [33].

Rhythm

Consider a stimulus which is composed of some pulses with some delays between them and therefore the participants can perceive them separately. This special stimulus is called rhythmic stimuli and the special type of these pulses and delays between them are called rhythm. In 1974 Gescheider studied two successive tactile stimuli on a participant's fingertip with a delay between them to obtain the minimum delay in which the participant was able to recognize these two stimuli separately. The minimum delay was approximately 5.5 milliseconds. Hirsh & Sherrick in 1961 conducted an experiment to investigate the temporal order of two stimuluses on two index fingertips of right and left hand of participant. They found that participant was able to perceive the temporal order by 75% when the minimum delay was 20 milliseconds. In 1990 Craig & Baihua proposed 3 results of judging of temporal order of stimuluses. Firstly, they studied the temporal order of two stimuluses with different patterns to the same fingertip by 12 milliseconds delay and it was the easiest one. When they used two fingertips of the same hand by 69 milliseconds, recognition was more difficult compare the first trial. The hardest one occurred when they applied these stimuluses on two fingertips of opposite hands (125 milliseconds) [33].

Locus

Locus or spatial location means locations on the human body. This vibrotactile feedback parameter shows different perceptions due to vibrations on different parts of the human body. Localization accuracy and recognition of patterns are two ways in which the sensitivity of the locus parameter is measured.

Measuring how accurately participants can perceive the vibration stimulus on different parts of the body is called localization accuracy. Geldard in 1960 investigated people's differentiation of vibration sources on the rib cage of the body and the result was 7 different positions. In 2003 Cholewiak & Collins studied the human recognition capability of different vibration parts on the arm. Without any specification localization, they found that the participants could perceive the vibration of seven different points where the accuracy was approximately 30-40%. As they close these seven points to the wrist and elbow the accuracy rate increased to 65-70%. Another related study was investigated the detectability of three vibration points on the arm by Brown in 2003, showed that the participants could distinguish the vibration points by accuracy around 95%. This shows that if the number of vibration locations decrease the accuracy recognition will increase [33].

The second way of measuring the sensitivity of locus parameter is recognition of patterns that means how accurately people can distinguish two different vibration patterns. To do this, Sherrick in 1964 introduced the masking effect which have two parts. Masking effect has two parts as temporal masking effect and spatial masking effect. If a vibration stimulus decreases the distinguishability of its successor, then temporal masking effect is occurred. But in spatial masking effect the vibration stimulus in one place will decrease the detectability another stimulus in another location [33].

2.2.3 Various tactile display devices

According to available tactile feedback devices in the market nowadays, it is possible to categorize them in 6 groups based on their specific respond to the human body and their operating principles. These 6 group technologies are: vibrotactile feedback, friction, surface shape, electrotactile feedback, non-contact feedback and hardness. Some of these technologies are just work inside laboratories but some came to market and doing well.

The most common device in this group which about all people have experienced it is mobile phones vibration that is generated by an actuator. To generate this kind of vibration the actuator must be attached under touch surface or attached to the mobile's body where the hand hold it. Therefore people can perceive the vibration on their fingertips or by their palm. To create this vibration, various types of vibration motors and actuators are used including: inertia actuators, voice coil motors, solenoid actuators, piezoelectric actuators and EAP which I explain them in detail along the applications that use them.

Vibration motors

As shown in Fig. 14, there are two types of vibration motors in the market. ERM and LRA are widely used in different technologies because of their characteristics of small weight, easy control and simple structure.

ERMs are DC motors which is attached to a shaft that carries an unbalanced (non-symmetric) mass. As DC motor starts to drive the mass also start to rotate thus a centripetal force is created. This force produces a small and rapid displacement that is known as vibration. One important point is that an ERM motor produces forces perpendicular to each other for instance in direction X and Z.

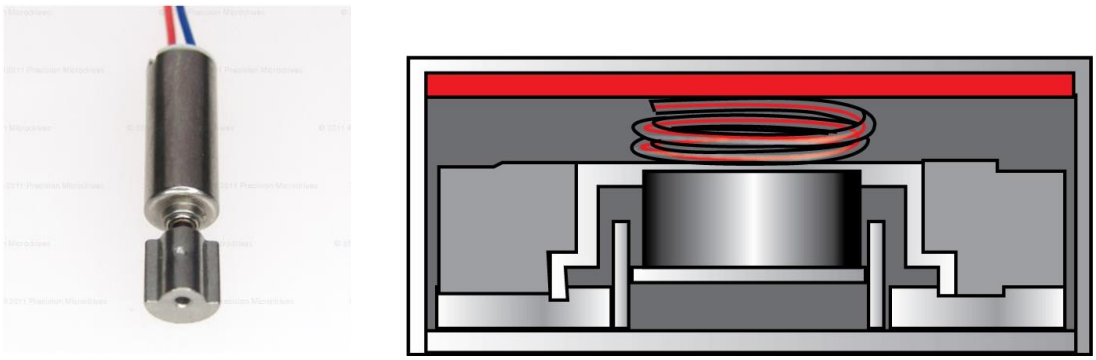

(a) **(b)**

Fig. 14. Two types of vibration motors. (a) ERM and (b) LRA.

In the other hand LRAs are composed of three important parts. A magnet, voice coil and a spring. A magnetic field that is produced by voice coil will excite the magnet thus it will move for instance up. Here spring will force the magnet to go down. This back and force

oscillation of the magnet around its normal position and in one plane will create the vibration.

For vibrotactile feedback devices three characteristics are very important to discuss such as frequency range, power drain and time respond. In Table 3 these features are compared between ERM and LRA.

Table. 3. Comparison of three characteristics of frequency, drain power and respond time between ERM & LRA. []

	Frequency	Power drain	Respond time
ERM	90-200 Hz	130-160 mA	30-50 ms
LRA	150-200 Hz	50-70 mA	20-30 ms

In Fig. 15 an ERM and a LRA and their vibration directions and their applications on the same device is illustrated.

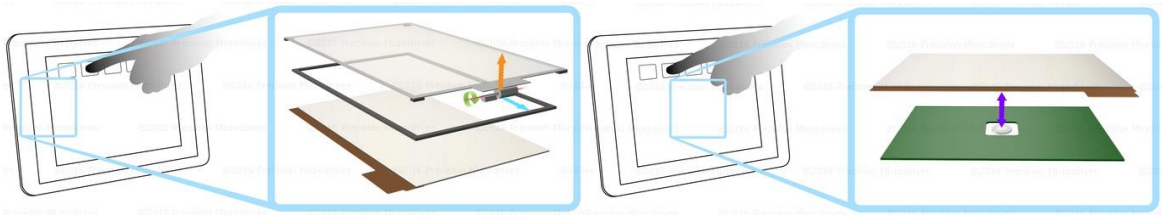

(a) **(b)**

Fig. 15. (a) An ERM motor that vibrates in X & Z direction while (b) a LRA motor that vibrate just in Z direction.

In 2010 Yatani & Troung [34] proposed a vibrotactile feedback device called SemFeel, with that the participant could able to perceive different semantic feedbacks when touch the screen. As it is shown in Fig. 16, five vibration motors are attached to the backside of a smartphone (up, down, right, left, and center) in a symmetric way.

Controlling all vibrotactile parameters they created eleven different patterns which can be categorized as positional, linear and circular. Using all these patterns except the clockwise

pattern, participants could increase their ability to detect the different buttons on the touch surface without looking at it up to 90%. Also they proposed 4 applications such as alphabetic keyboard, calendar application, a maze game and a web browser for people with visual impairment.

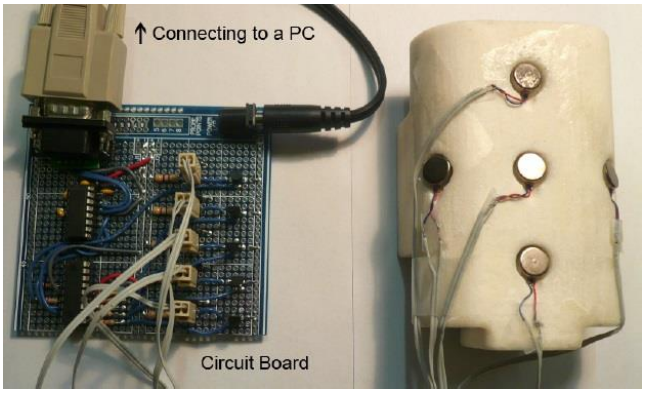

Fig. 16. The SemFeel prototype: the circuit board and five vibration motors that is attached to the backside of a mobile touch screen. [34]

Ubi-Pen, Fig 17, is the name of a safe, silent, light, fast and low power dissipation vibrotactile device which was created by Kyung, Lee & Park [35] in 2007 based on the idea of pen-like haptic. It produced three different groups of texture and also vibration feedback which are demonstrated in Fig. 18. In order to simulate these texture patterns on a pen, they used a 3x3 pin-array tactile display which was powered by a very small ultrasonic linear motors 'TULA35' which were created by Piezoelectric Technology Co.

Fig. 17. A user hold a Ubi-Pen. [35]

The first group of textures were characterized by directions of gratings. Second group were

those textures that were characterized by groove width and the participant could feel horizontal grating during rubbing the surface. Last but not least were those textures that characterized by their shapes.

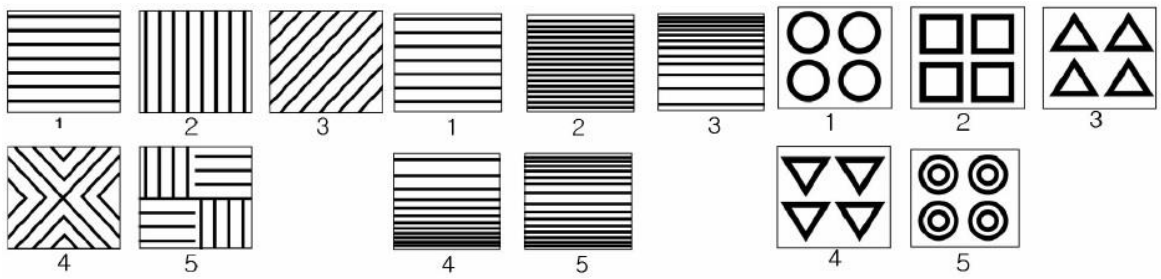

Fig. 18. Three groups of texture (a) direction of gratings, (b) groove width, (c) shapes. [35]

Voice coil actuators

Voice coil actuators like other actuators produce force and displacement. The structure of a voice coil motor is based on a copper coli which is energized by an electric current alongside the magnetic field that widely produced by a permanent magnet. Thus this force is proportional to the electric current and magnetic field. These devices are used in linear and rotatory applications which create force and torque as output respectively. High acceleration and high frequency oscillation applications are other aspects of using these non-communicated devices. Compare to ERMs voice coils have a smaller latency, therefore they can be applied where a faster tactile feedback is required.

In 2001 Fukumoto & Sugimura [36] proposed Active Click as a tactile feedback for touch panel. According to Fig. 19 the actuator were attached to the PDA's body or to the backside of touch panel thus the participants could perceive the vibration on palm or tapping on the fingertip. For creating these feedbacks on palm and fingertip a single pulse or short burst is supplied to the actuator. They decided to use a voice coil actuator instead of ERM since the control of voice coil is more suitable than ERM.

The idea of Tactons or tactile icons as structured tactile messages for non-visual information display, was invented by Brewster & Brown [37] in 2004. They used a wide range of vibritactile parameters such as frequency, intensity, duration, rhythm and spatial location. Later they added the roughness as new parameter to Tactons. They have this

ability to be used in different interfaces including for blind people or in mobile and wearable devices. Participants perceived these vibration feedbacks with accuracy success of 71% in overall. However these perception rate was 93% for rhythm and 80% for roughness.

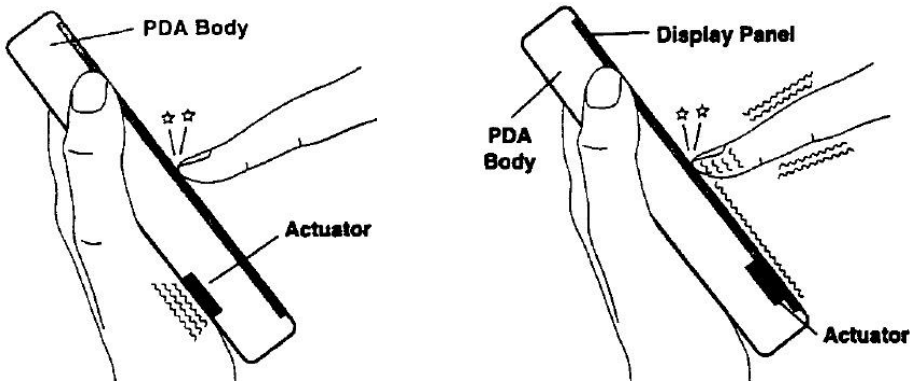

Fig. 19. Active Click. (a) Body mounted actuator and (b) panel mounted actuator. [36]

In 2006 Brown, Brewster & Purchase [38] proposed a calendar application using multidimensional Tactons which could produce vibrotactile feedbacks by association of rhythm, roughness and spatial location. The idea was that participants should recognize the type of appointments (meeting, lecture, tutorial) using three different rhythms (7 pulse, 4 pulse,1 pulse), importance of appointment (smooth, rough, very rough)by three distinct roughnesses (250 Hz, 50 Hz, 30 Hz) and finally the time until appointment by three equidistance locations on the wrist, elbow and somewhere between them.

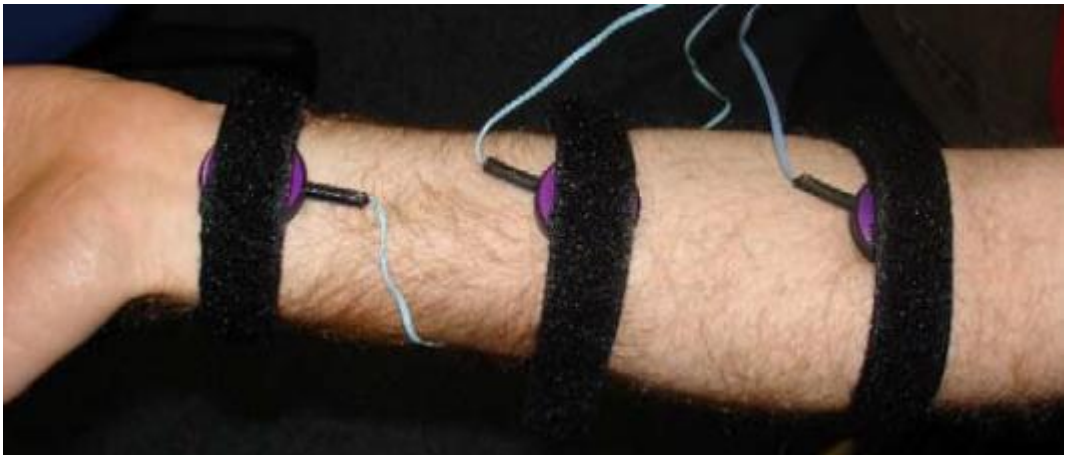

Fig. 20. The location of Tactors on the participant's forearm.

Solenoid Actuators

For producing small displacements motion control both technologies, voice coil actuators and solenoids, are useful but according to Table 4 there are crucial differences between them that force engineers to be careful when choose one over the other.

Table 4. Comparison between voice coli actuators and solenoid technologies

	Voice Coil	***Solenoid***
Force	Low to medium	High
Stroke	5 inches maximum	¼ inches maximum
Constant Force	Yes	No
Reversible	Yes	No
Position/Force Control	Yes	No
Cost	Moderate	Low

Since the structure of voice coil actuators were discussed in last section, here it worth to know about solenoid's structure. A solenoid is composed of a coil with no magnet attached to the steel or iron core housing and also a spring. When electrical current flows to the coil, a magnetic field is created and consequently this force will displace the iron core. When the power is turned off, the force will drop to zero and the spring will push the iron to its original position.

In 2009 Yang et al. [12] proposed a miniature pin-array tactile module that could produce vibration feedback using the idea of solenoid actuators. Their new proposal was consisted of a coil, permanent magnet, contactor and a spring as shown in Fig. 21.

Based on the output force of contactor and also the actuator's wide range of frequency they constructed a 3x3 pin-array that could stimulate fingertip's Pacinian mechanoreceptors and provide various tactile sensations. The total size of this miniature device was 15mmx15mmx8.8mm and its weight was 8g. The contactors can be stroked around 0.2 mm and in a wide range frequency. Power consumption of actuators is another crucial point which for 1 Hz is 0.16 W and for 340 Hz is 0.39 W thus it is low power consumption device. Minimum activation force to stimulate the hand's mechanoreceptors is 3.6 mN.

Theses contactors could produce a force of 5 mN thus it is more than the finger's threshold.

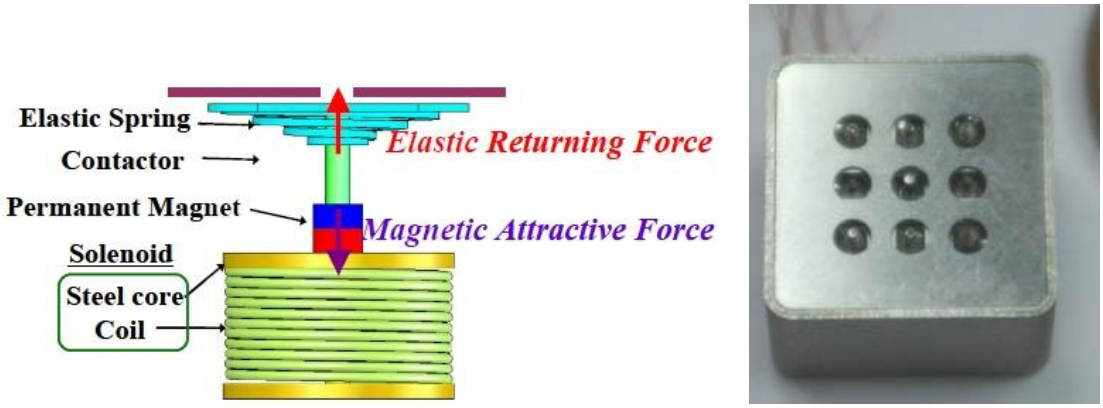

(a) **(b)**

Fig. 21. (a) Different components of tactile actuator, (b) pin-array tactile module. []

Piezoelectric actuators

Piezoelectric actuators are invented based on inverse piezoelectric effect. But what is piezoelectric effect? When certain solid materials such as crystals and some ceramics are applied under mechanical stress, in response they will create an electric charge. This process is called piezoelectric effect. The word piezoelectric is driven from two Greek words. The origin of piezo is Greek word *peizein* which means press or squeeze and electric is driven from Greek word *elektron.*

The main characteristics of piezoelectric effect is its reversibility. It means piezoelectric materials can generate electric charge when are applied to an external stress (direct piezoelectric effect). In the other hand these materials can exhibit inverse piezoelectric effect that means an outer electric charge can stretch or compress the material which is applied in piezoelectric actuators. Piezoelectric actuators have three significant features with them can overcome the other actuators including fast respond, thin physical structure and wide range frequency. Therefore in applications that have thin and large surfaces, piezoelectrics are the best choice as I will discuss some of them in below.

In 2002 Poupyrev et al. [14] invented a thin, miniature and low power tactile actuator

named TouchEngine, Fig. 22, which was able to be embedded under surface of a mobile phone and crate wide range of tactile feedbacks from simple clicks to very complex vibrotactile patterns.

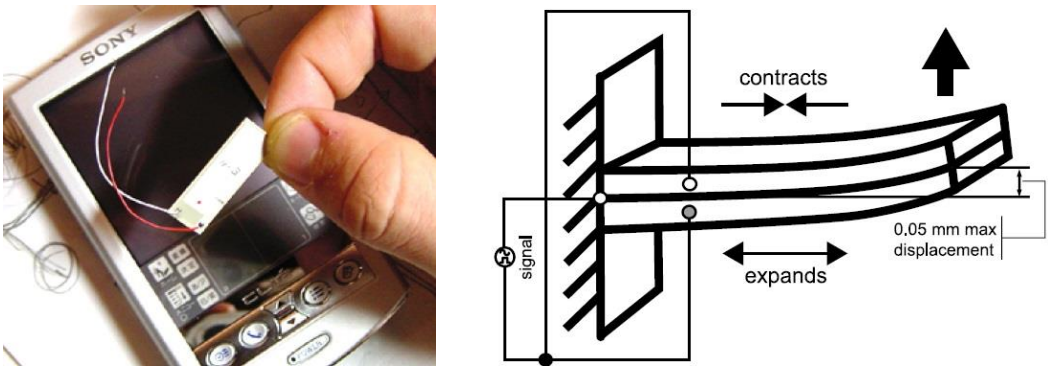

(a) **(b)**

Fig. 22. Ambient Touch: (a) TouchEngine actuator, (b) the bending motor. [14]

Structure bending of TouchEngine actuator will lead to a very small displacement around 0.1 mm. This is a point of challenge since a very negligible mechanical motion must provide a detectable force and therefore a significant vibrotactile on participant's skin. To solve this obstacle, inventors proposed two solutions; direct tactile display and indirect tactile display.

The idea of direct tactile display is that an actuator vibrate a single part of the device like a button or whole surface of the device therefore participants will recognize different vibration patterns. This seems very difficult and expensive if each single part of the device needs its own piezoceramic actuator.

In indirect tactile display, they embed the actuators anywhere inside the tactile device with a small weight attached to it. Since for this isolated system there isn't any external force, the total momentum is zero thus the final force can be calculated using conservation momentum formula. As the actuator bends and consequently the attached mass to it moves up and down with momentum P(a), the momentum P(d) of whole device is produced which is equal but in opposite direction. According to the second Newtown's law of motion, the higher the actuators' acceleration the stronger the output force and eventually

this will lead to a more recognizable tactile vibration on people's skin.

Later in 2003 Poupyrev & Maruyama [13] introduced a tactile interface for small touch screens. They embedded four TouchEngine actuators in the corners of a Sony's Clie PDA touch screen between the TFT display and the touch sensitive-glass which is demonstrated in Fig. 23.

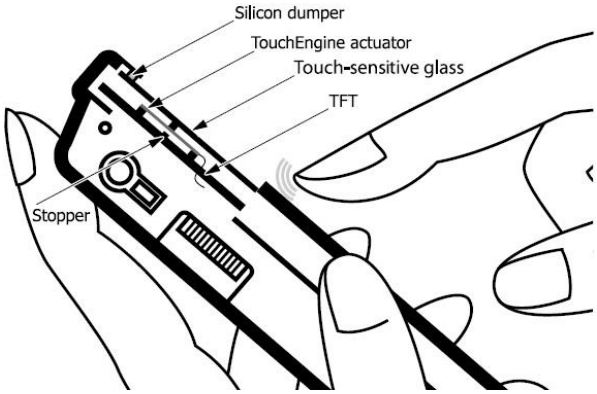

Fig. 23. Small touch screen using TouchEngine actuators. [13]

This device is based on five advantages including: actuation of the touch screen. Localized tactile feedback, small-high speed displacement, silent operation and last but not least reliability. Below I will describe these important characteristics.

1) Actuation of the touch screen: These four actuators are very thin (0.5 mm) therefore can be placed inside the interface between a heavy TFT layer and a lightweight glass display. When a sufficient voltage is applied to the device, the actuators start to move up and down rapidly and vibrate the lightweight touch-sensitive glass not entire device. This leads to producing a wide range of sensation feedback on participant's fingertip. Also the actuators do not increase the distance between TFT and glass layers therefore during the time the precise of vibration feedbacks won’t decrease.

2) Localized tactile feedback: As shown in Fig. 23 a soft silicon damper is placed between the glass layer and the frame ridges. Thus the participants perceive the localized vibration on their touching fingertips not on their entire hand. The other reason is protecting the device from dust.

3) Small-high displacement: Displacement of these four TouchEngine actuators is very small around 0.05 mm. But since their acceleration is high, they are able to produce significant and detectable vibrotactile sensations.

4) Silent operation: Noisy device and environment decreases vibration perception. By implementing proper waveform and mechanical design, it is possible to reduce the noise.

5) Reliability: In Fig. 23 there is a stopper installed under the actuator. The reason is that when a fragile actuator bends more than 0.1 mm up or down, occurring a bad damage to the device is quite possible thus the stopper resists against high bending.

Electroactive polymer actuators

Electroactive Polymers (EAPs) are polymers which can produce a deformation in size or shape when are applied under an electric field therefore they are used widely as actuators and sensors. Compared to piezoelectric materials that are widely used as actuators, EAPs can produce a large amount of deformation in their size and shape thus can be applied in the fields like haptics and robotics.

Shin et al. [39] in 2012 proposed a tactile feedback for a button GUI on a touch device that used EAP very thin actuators which exhibit a high displacement, low input voltage and low weight. They found that three parameters such as rapid respond time, short falling time and patterns in response to touch and release of button, are very important for simulation of true feeling of physical button clicking.

This EAP film actuator was measured about 34x38x0.5 mm and its respond time was 5 ms. The frequency range was from 40-300 Hz and elongation of the device happens when a sufficient voltage is applied 0 to 3.3 -V.

They produced many tactile patterns but just these six above mentioned patterns were detectable and had realistic button clicking. As shown in Fig. 24 patterns are constructed based on a simple impact (10 ms/100 Hz) and a vibration impact (40 ms/200 Hz). All the patterns also are applied under a 3.3 V input voltages.

Surface shapes

Dynamically changeable physical buttons on a visual display was an idea for perception

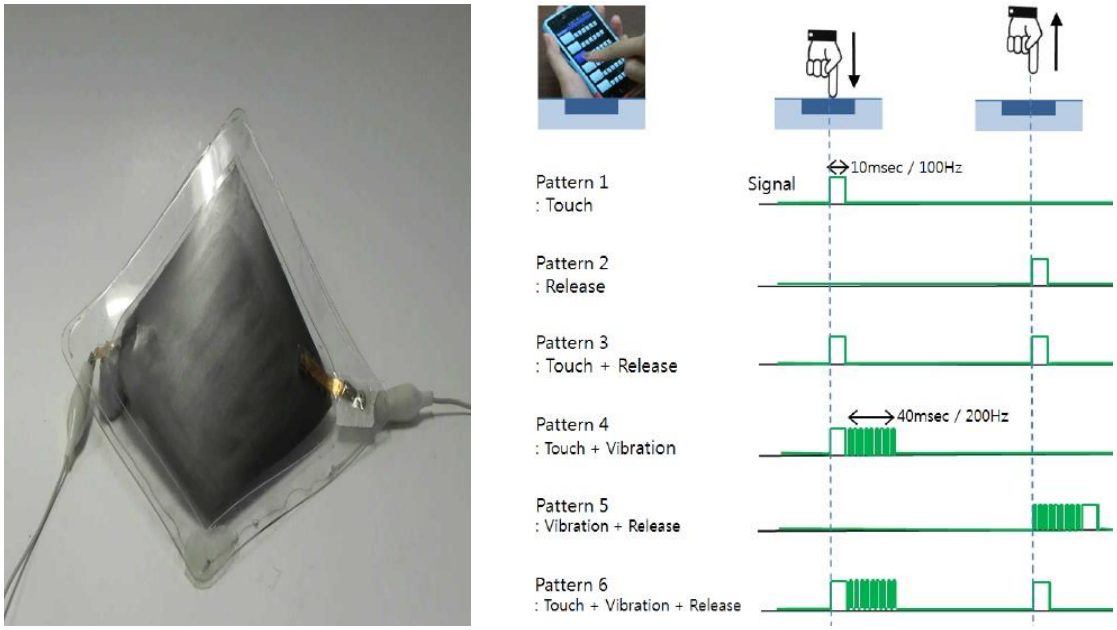

(a) **(b)**

Fig. 24. (a) Electroactive polymer prototype, (b) simulation of button tapping. [39]

different shapes on the surface which was proposed by Harrison & Hudson [40] in 2009. They used the pneumatic actuation idea in their device for some reasons including: 1) it was an integrated display, 2) it was a cheap interface since the composed materials (acrylic, glue, and latex) were simple and there were no need to special actuator for every vibrotactile feedback. Also physical actuation elements were constructed in a way that do not require any motors, wires and conduits.

As it is shown in Fig. 25 they constructed an air chamber using several layers of acrylic and a translucent latex on top of them as a deformable projection surface. Actuation could occur by negatively and positively pressurized air chamber when the air flew in by a small pump attached to it. In the figure acrylic materials are shown in grey, adhesive in blue and latex in green.

When a negative pressure is applied to the air chamber, the latex deforms inward and a concave feature is produced. In the other hand, as air flows inside the chamber and the chamber is positively pressurized, convex patterns is created. Therefore by cutting

different shapes on the blue layer, participants could perceive variety of shapes by touching the surface.

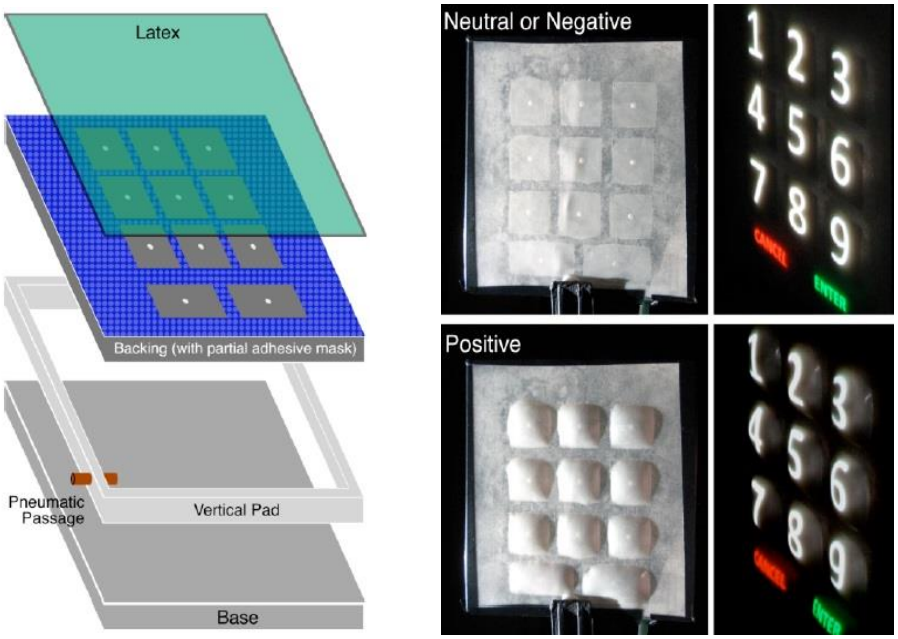

(a) **(b)**

Fig. 25. (a) Different layers of air chamber, (b) surface shapes create haptic feedbacks on screen. [40]

Hardness

In 2010 Jenson e al. [41] in RWTH proposed MudPad as a localized tactile feedback and haptic texture on multitouch screen. Time response of MudPad is very short therefore it can create instant multi-point feedback for multi-touch input and consequently is able to produce dynamically changeable textures.

As shown in Fig. 26, MudPad is composed of four layers. The ground layer is a set of electromagnets that can be magnetized individually to produce a localized magnetic field. A resistive high-resolution multitouch surface is placed on the grounded layer. On top of touch surface, there is a pouch shape surface full of Magnetorheological (MR) fluid which is covered by soft sheets on both sides. The outer layer of MudPad is a latex cover. The pouch in third layer is filled by a magnetic fluid that is categorized as a smart materials. By applying a magnetic field on this fluid, its viscosity can be controlled. When a magnetic

field is applied to the device the particles of liquid are aligned with the axis and increasing the viscosity. As soon as the magnetic field is removed, the particles will come back to their original position and the viscosity will be decreased.

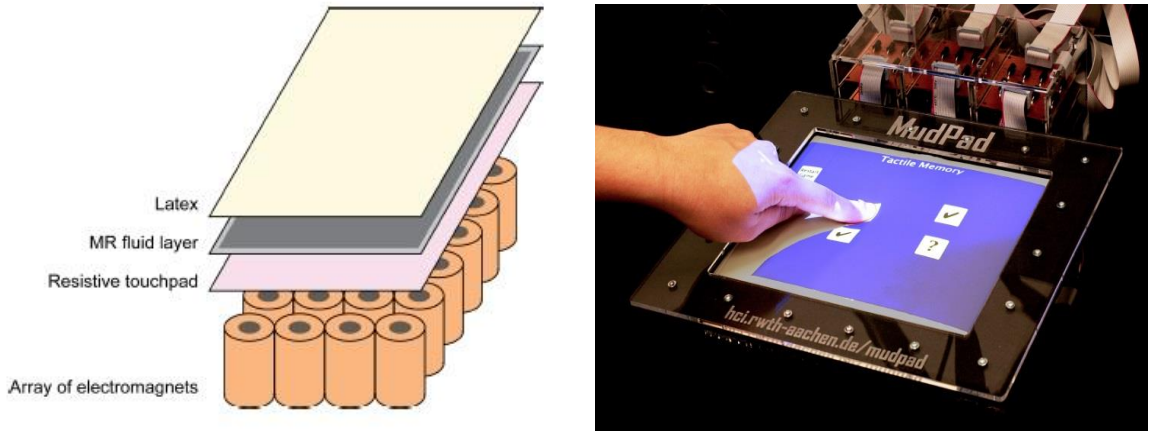

(a) **(b)**

Fig.26. (a) Four different layers of MudPad, (b) MudPad prototype. [41]

Time response of alignment and realignment of MR fluid is approximately 2 ms which is considered as very quick. Also MudPad can cover a wide range of frequencies up to 600 Hz and create arbitrary waveforms. Based on these facts MudPad is able to produce various localized haptic textures on the surface in real time.

Non-contact surface Haptics

Carter et al. [42] invented Ultrahaptics as a multi-point mid-air tactile feedback for touch surfaces. This interactive screens project the haptic patterns on mid-air using focused ultrasounds, directly onto participant's hand without touching tools, attachments or surface itself. Whole process is based on the idea of *acoustic radiation force* which is producing a force on a target in mid-air using an array of ultrasound transducers as in Fig. 27.

Finding an alternative to stimulate human skin's receptors without physical contact by focused ultrasound, was investigated in 1970 and it was showed that inducing tactile, thermal, tickling, itching and pain sensation is possible. There are two solutions for vibrating the fingertip's mechanoreceptors by ultrasound. In the *acoustic radiation force*,

the ultrasound is focused onto the skin's surface and induces a shear wave in the skin tissue. Therefore a displacement is occurred which leads to excitation of mechanoreceptors. In the second approach, the ultrasounds bypass the mechanoreceptors and directly vibrate the nerve fibers but since it requires a powerful acoustic field, in most of application the first approach is used.

Fig. 27. Creating haptic feedbacks on a target (hand) in mid-air using ultrasound transducers.

By triggering ultrasound transducers with specific phase delays, many ultrasound waves flow above the surface and displace the air to create a different pressure (*acoustic radiation force).* All these ultrasound waves arrive at a focused point concurrently as a target which has a different pressure. Thus the participant perceive it as vibration stimuli on the skin. By changing the frequency and use different pulses it can provide a wide and rich set of textures.

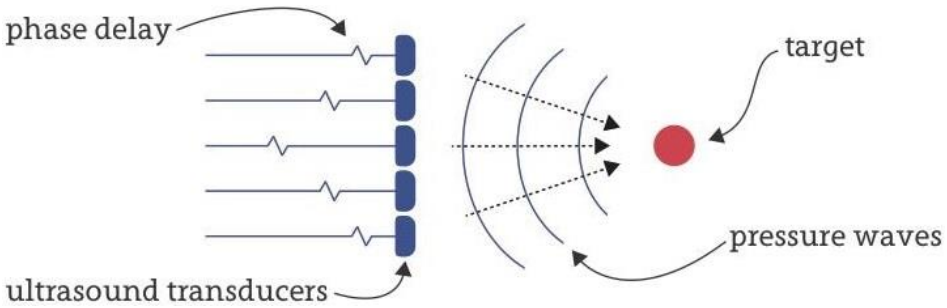

Fig. 28. Acoustic radiation force process in which a pressure is created on a target in mid-air by phase delayed ultrasound waves.

Electro-tactile feedbacks

Altinsoy & Merchel [43] in 2012 proposed an electrotactile display on a touch screen which can provide haptic sensations on the user's fingertip by transmitting a small amount of electric current through electrodes to the skin. Being a silent device, having good contact with skin, not having moving components and capability of excitation for static and dynamic contact are mentioned as their advantages. According to previous studies electrotactile stimulations can directly vibrate the mechanoreceptors and therefore create feedbacks such as vibration, buzz, pulsation and pressure. According to the Fig. 29 two electrodes are attached on top (optically transparent) and rear (electrically conductive) of the handhold device. Now if participant touches electrode 1, a small amount of electric current flows into his skin and excite the mechanoreceptors in the fingertip thus a haptic sensation is produced. This electric current flows the whole body and is distributed on electrode 2 which is largely contacted with other hand thus user does not sense a tactile sensation.

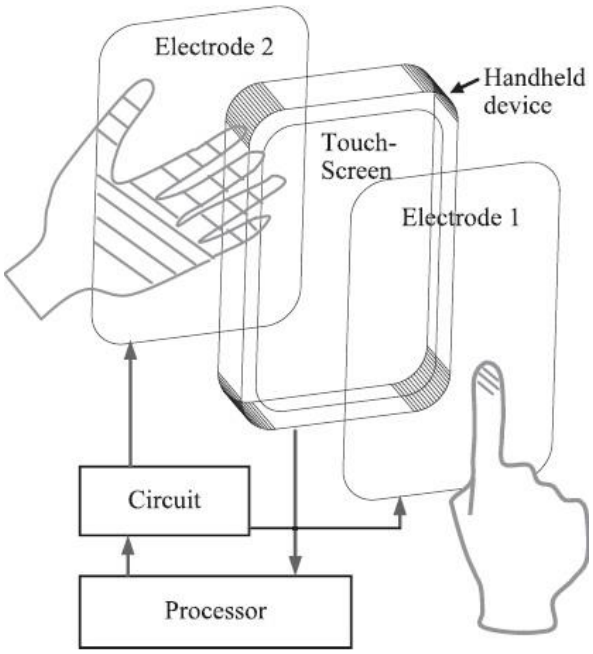

Fig. 29. Creating electrotactile feedback on participant’s finger using two electrode that are attached on a handhold device. [43]

Friction

When the finger moves on the touch screen a friction is produced between the fingertip and the surface according to physics laws. By changing the friction on the surface it is possible to produce different textures. Therefore users can perceive the texture when they draw a picture or move a file on the surface in real time. People have tried to bring into the picture this idea in recent years by using three solutions including: 1) Reducing friction coefficient, 2) Increasing normal forces, 3) Producing lateral force on the fingertip.

1) Reducing friction coefficient

One of the most significant solutions to reduce the friction between fingertip and surface is *squeeze film air effect* which is shown in Fig. 30.

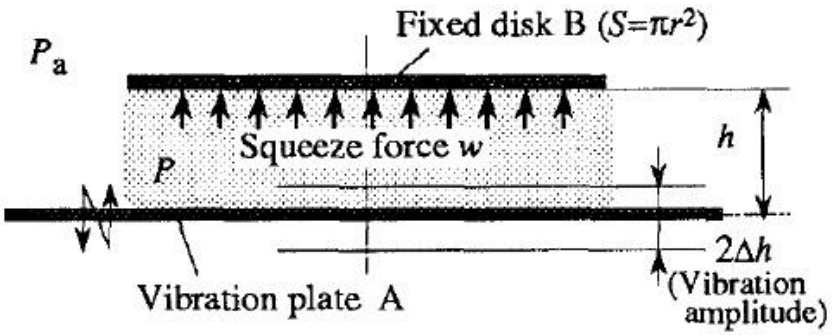

Fig. 30. Squeeze film air effect between two plates. [44]

When the distance between vibration plate A and fixed disk B, *h* as mean clearance, is sufficiently smaller than the size of top disk B, and also the vertical frequency vibration of plate A is high enough, the pressure between two plates *P* becomes higher than the around pressure *Pa*. Consequently disk B feels floating since it is applied by an upward *squeeze force w*.

Watanabe & Fukui [44] in 1995 used a vibrating Langevin-type piezoelectric actuator to create ultrasonic vibration which leads to *squeeze film air effect* and therefore control the tactile sensation of surface roughness as demonstrated in Fig. 31. The key feature in this proposal is that the actual surface configuration does not change at all but the tactile sensations are altered. By changing the amplitude of ultrasonic vibration, they produced

various tactile sensations such as roughness and smooth perception.

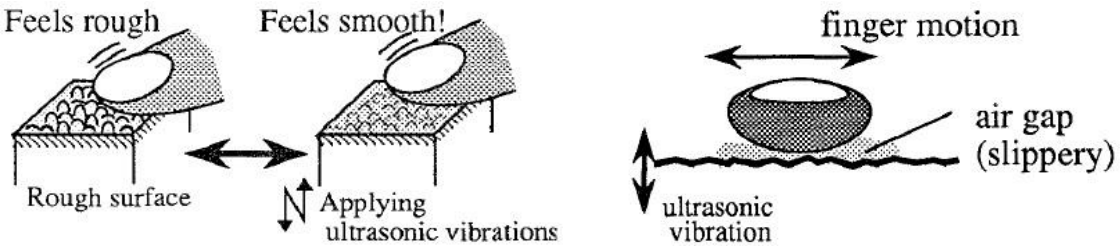

(a) **(b)**

Fig. 31. (a) Squeeze film air effect provides smooth sensation on fingertip, (b) motion of finger on the squeeze film air which is created by ultrasonic vibration. [44]

They held an experiment with two conditions for perceiving the tactile feedbacks using ultrasonic vibrations. Condition 1 was a well-finished flat surface and condition 2 was a rusty rough surface. Three parameters were the same in both conditions: steel material surface, vibration amplitude of 2 μm and vibration frequency of 75.6 kHz. Participant's answers to questions about description of tactile feelings of the surface were approximately the same as shows in Table 4.

Table 4. Comparing the sensation of surface without and with squeeze film air effect.

Case	**Tactile Impression**	
	Without vibration	**With vibration**
i)	fat but sticky	slippery as with an air layer
ii)	rough	smooth less slippery

2) Increasing normal force

Increasing normal force between touch screen and the finger moving on it, is based on the idea of *electrovibration effect* which is created when a dry finger moves on a conductive surface which is covered by a thin insulator and applied by 110 V, the participant feels a rubbery sensation. This phenomenon can be explained as below: a dry moving finger on the conductive surface which is excited by a voltage, form a capacitor. The finger's

insulating dry outer skin is dielectric layer where the conductive surface and the fluid under finger's tissue will be two opposing plates. Applying a DC voltage on conductive surface produces an attraction normal force between the surface and the finger. This attraction force is too weak to be perceived by human body when the finger is static but as soon as the finger moves on the surface, alternating friction between surface and hand provides rich rubbery sensations.

But we should care about the differences between *electrocutaneous, electrostatic* and *electrovbibration.* In *electrocutaneous* process, electric charge passes through the skin and stimulate finger's mechanoreceptors. *Electrostatic* phenomenon uses an intermediate object such as aluminum foil on an electrode pattern that is applied by a periodic signal. By applying the voltage, a weak electrostatic attraction is produced between the object and the electrode that is perceived on finger as various haptic feedbacks. In *electrovibration* there is not a passing electric charge through the skin. Electric charge is induced by conductive surface to the finger that is moving on it.

TeslaTouch which was proposed by Bau et al. [6] in 2010, used the idea of *electrovibration* to control electrostatic friction between a touch screen and the finger. It provides a wide range of sensations on the finger that is moving across the surface. Two important advantages of TeslaTouch over other haptic devices is that it does not need mechanical actuators and also it does not have moving parts. As shown in Fig. 32 TeslaTouch is composed of a transparent electrode sheet on top of a glass plate and coated with an insulating layer. When a periodic voltage V(t) with a sufficient amplitude is applied to the electrode, a normal attractive force f(e), electrically, induced between the surface and moving finger thus a dynamic friction f(r) is provide. Since f(e)'s amplitude changes with periodic signal therefor friction f(r) also is dynamic and it leads to a periodic haptic feedbacks when finger moves on surface.

They held five experiments about the stickiness (sticky to waxy), smoothness (bumpy to smooth), fineness (coarse to fine), pleasure (pleasant to unpleasant) and level of friction vs. Vibration. In each experiment there were four situations as below: 1)400 Hz, 115 Vpp, 2)400 Hz, 80 Vpp, 3)80 Hz, 115 Vpp, 4)80 Hz, 80 Vpp. Participants perceived low frequency stimulus as rougher than high frequencies. In high frequency textures, increasing

in amplitude perceived as smoothness and in contrast in low frequency stimuluses increasing in amplitude was sensed as stickiness.

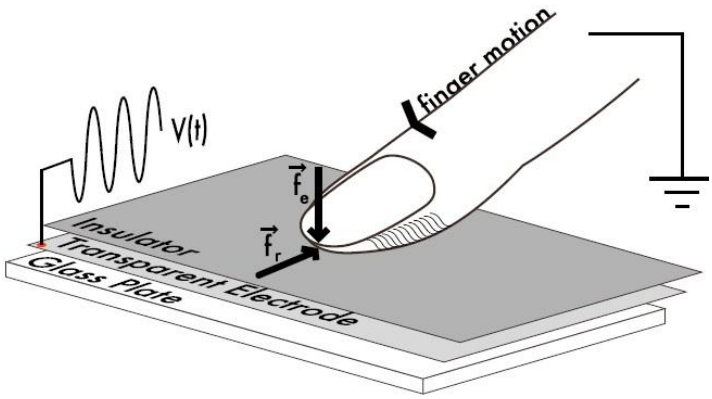

Fig. 32. A normal force is created on the finger while finger moving on the TeslaTouch surface. [6]

In 2017 Wang et al. [45] proposed EV(2)-Pen based on *electrovibration* and *vibration* haptic feedback. *Electrovibration* technology produces multisensory feedbacks as the pen is moving on the surface while the *vibration* technology is responsible for coating haptic sensations at stationary conditions.

As shown in Fig. 33 they used a 32 inches monitor for displaying while for capture the finger's input installed a 32 inches IR multi-touch frame. The pen has 100 mm length, 7 mm width and 5 mm pen-tip.

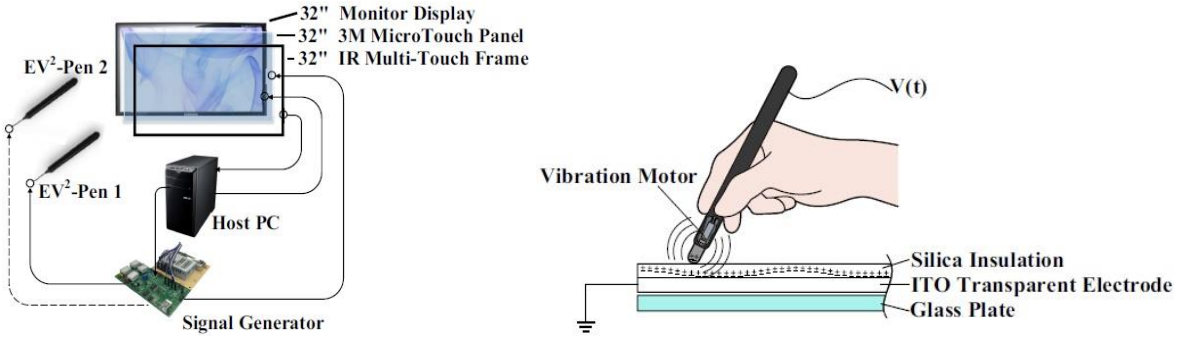

(a) **(b)**

Fig. 33. (a) Structure of EV2-Pen, (b) different parts of EV2-Pen. [45]

Since it uses two technologies including *electrovibration* and *vibration*, for each there is a different set up which is explained here:

Electrobibration feedbacks:

To activate *electrovibration,* the pen is connected to a signal generator and also to a 3M micro-touch panel. According to Fig. 33, 3M micro-touch panel is composed of an ITO transparent electrode sheet on top of a glass plate and coated with a silica insulation layer. The device is capable of producing a wide range of frequency from 10 Hz to 1 KHz along the amplitude range of 0 V to 400 V with a current limited to 0.5 mA. When the pen slides on the surface, an electrostatic attraction force is produced which increase dynamic friction between pen and underlying electrode. This dynamic friction can be manipulated by controlling the waveforms, frequency and amplitude and therefore provides a wide range of haptic sensations.

Vibration feedbacks:

For these feedbacks a motor (2.0 V to 3.0 V, LA4-503AC2) of 4.3 x 10.7 mm is mounted inside the motor while 15 mm from pen-tip. The signals of this motor is controlled by the microcontroller.

3) Producing lateral force

In previous demonstrations related to surface friction, people reduced coefficient of friction by the idea of *squeeze film air effect* and increasing normal force using *electro vibration* phenomenon. In both process, haptic feedbacks produced by playing with friction between the surface and participant's finger. In producing lateral force, people use the idea of creating friction between surface and finger when touch surface is moving under fingertip.

Chubb et al. [46] in 2009 introduced ShiverPad as a glass haptic surface which creates shear force on a bear fingers. The core part of the ShiverPad is a TPaD [47]. TPaD uses ultrasonic vibrations (39 KHz signal is generated by a waveform generator chip and amplified to 40 V using an audio amplifire) to create a squeeze film of air between the finger and touch surface to modulate friction between them. The main idea behind of ShiverPad is to oscillate the TPaD in the horizontal (in-plane) plane by voice coil actuator

with frequency of 20-100 Hz when alternating between low and high friction at the same frequency. As shown in Fig. 34, when the TPaD moves in one direction the squeeze film air is turned off thus the high friction state is produced. In the opposite direction, the squeeze film air is turned on and the friction between finger and glass surface is reduced (low friction). At high voltage coefficient friction was μ=0.15 while at zero voltage it was μ=0.95. Later in 2010 [48] the same group increased the in-plane frequency to 854 Hz thus producing a net-force of 80 mN to display a virtual toggle and virtual edges. Results showed that participants could perceive the virtual edges.

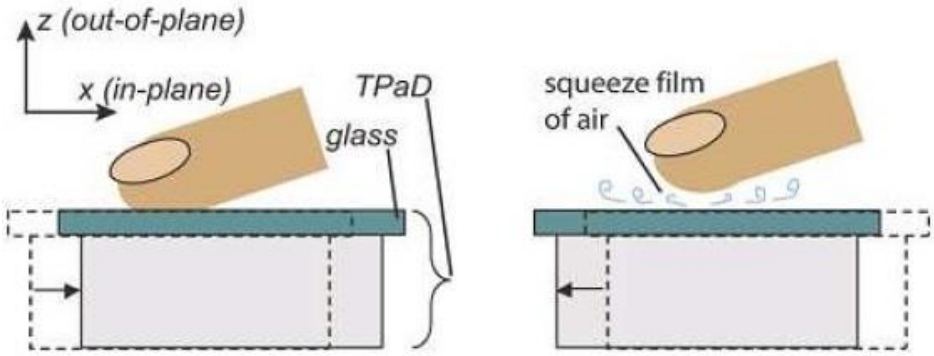

(a) **(b)**

Fig. 34. (a) Producing high friction while squeeze film air is turned off and (b) low friction when squeeze film air is turned on. [48]

In 2012 Dai et al. [49] proposed LateralPad, Fig. 35, as a new developed version of ShiverPad. In contrast with ShiverPad, LateralPad uses piezoelectric actuators for exciting the glass surface both in-plane and out-plane with the same frequency of 22.3 KHz. The output force is 70 mN which is not very perceivable for human body.

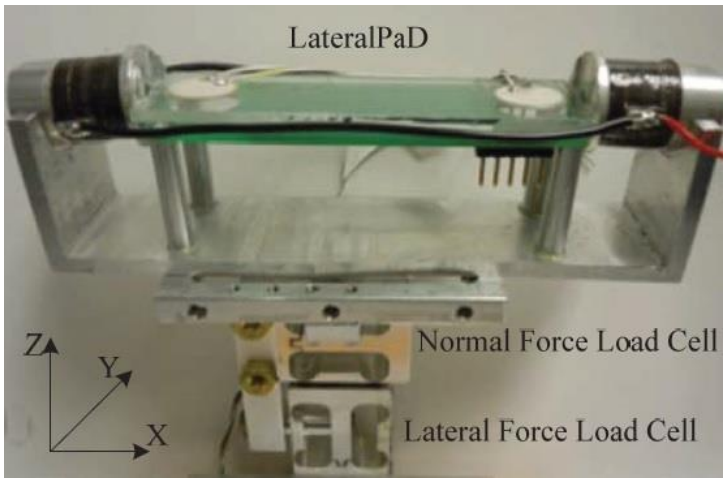

Fig. 35. LateralPad which provides haptic sensations using piezoelectric actuators in both horizontal and vertical vibration. [49]

3 RESULTS

3.1 MSM effect-based actuator

The pulse MSM actuators which we used in our prototype were designed and modeled by Sozinov & Tellinen, assembled by Huimasalo and characterized by Saren & Musiienko in Material Physics Laboratory at Savonlinna.

3.1.1 MSM actuator design

As shown in Fig. 36, the actuator is composed of three parts including:

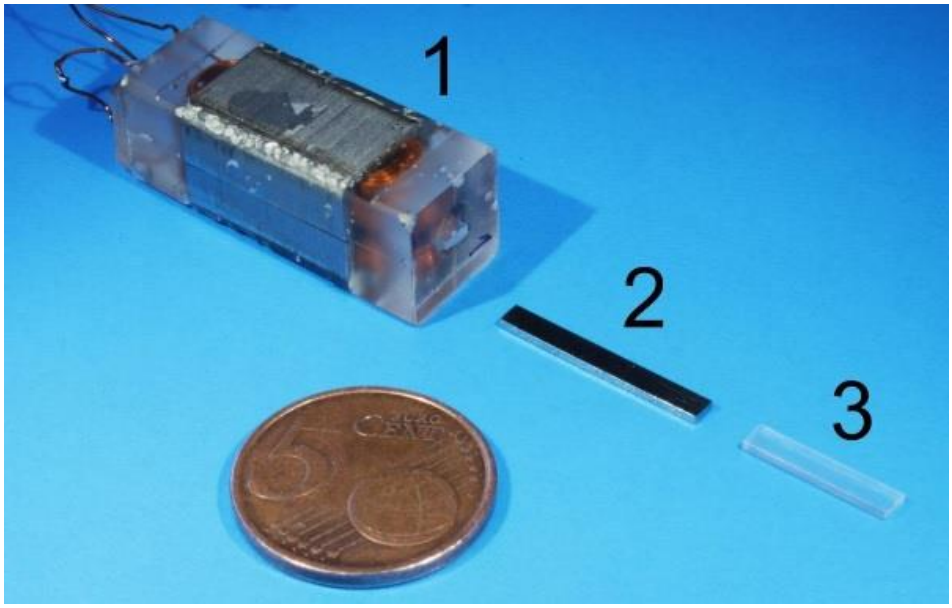

Fig. 36. Different parts of MSM actuator.

1) Tow coils of wire are connected in series and construct a magnetic core with windings, 2) A bar of Ni-Mn-Ga element with the size of ~1x2.2x20 mm(3) that has an active part of ~18 mm inside the core and 3) A plastic stick to connect the active element to a load.

The above mentioned active element of actuator is a piece of Magnetic Shape Memory (MSM) alloy Ni-Mn-Ga which is categorized as smart materials that change their shape as applied under a moderate magnetic field. In this actuator the used MSM alloy is a Ni-Mn-Ga 5m martensite that can produce a strain of 6% in a moderate magnetic field of ~0.7 T. The output force is in the range of 1-2 N per millimeter cross section. Maximum stroke of this 18 mm active element is around 1mm which in compare to other actuators in

market such piezoelectric is quite large.

Firstly the active Ni-Mn-Ga element by its contracted state is adjusted inside the core as having its easy and shortest axis of magnetization aligned along its length using accurately pushing the plastic stick. Current pulse creates a saturation magnetic field applied to the element's largest dimension perpendicularly. The field aligns the easy (and shortest) axis along the small dimension of the element thus the element is elongated.

Two mechanisms are possible to return the MSM element to the contraction state, either using a magnetic field source to produce a magnetic field along the element or a mechanical stress like a spring force to contract MSM bar.

Push-push design actuators is an idea in which two actuators are working against each other in a way that activation of one actuator provides restoring force to contract the second one.

Each of two coils which are used inside the actuators have 60 turns of 0.3 mm insulated copper wire. In Table 5 and 6 windings characterization is discussed with and without element inside the actuators.

3.1.2 Actuation characterization

They put a metal weight of 102 g as a load in front of the actuator directly in contact with plastic stick to measure the actuator response to magnetic pulse. When the actuator was in fully contracted state they used a square shape current pulse of a duration of 10 ms and amplitude of 4 A. The current was generated by a bipolar power amplifier (KEPCO BOP 100-4DL4886) connected to a waveform generator (Aim-TTiTGA12104). During the actuation the metal weight was sliding on a metal surface and they measured the velocity of the weight using a Doppler Vibrometer (Polytec OFV-5000, OFV-534).

Table 5. Winding characterization without the element.

	Measured at 100 Hz		**Measured at 300 Hz**	
	Inductance, mH	**Resistance, ohm**	**Inductance, mH**	**Resistance, ohm**
Actuator #1	1.246	1.644	1.246	1.655
Actuator #2	1.283	1.618	1.283	1.630

Table 6. Winding characterization with element inside.

	Measured at 100 Hz		**Measured at 300 Hz**	
	Inductance, mH	**Resistance, ohm**	**Inductance, mH**	**Resistance, ohm**
Actuator #1	1.246	1.644	1.246	1.655
Actuator #2	1.283	1.618	1.283	1.630

In the Fig. 37, time versus coil's voltage and current during the actuation of Actuator #1 is showed. Actuator #2 also pursues the same behavior.

Time dependence of coil' power of both actuators are shown in Fig. 38. A current with the characteristic rise time (from 10% to 90%) of 230 μs is generated by power supply. Also as shown in figure...the average power generated (in middle part of the pulse) by Actuator #1 is ~26 W and for Actuator #2 is approximately 22 W.

In Fig. 39 the velocity of two actuators are measured versus time which do the same behavior. The metal weight in front of the actuator is accelerated to its maximum at 0.17-0.2 m/s for actuators within duration of around 6-7 ms while the full stroke of 0.8-0.9 mm is provided. After reaching maximum velocity the metal weight continues its journey away from the actuator but the velocity is slow down since since the friction between weight and surface is increasing.

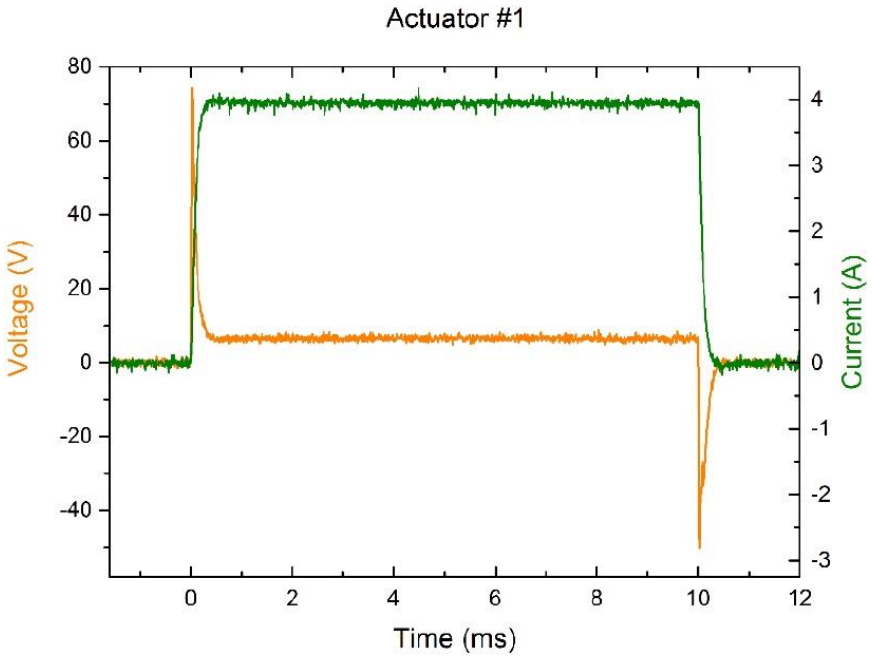

Fig. 37. Voltage and current versus time measured for Actuator #1.

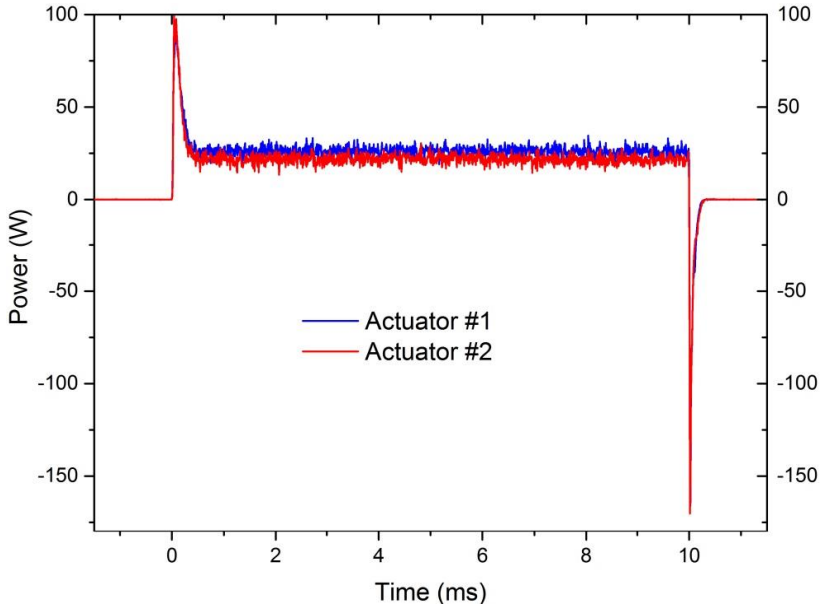

Fig. 38. Power versus time calculated for both actuators.

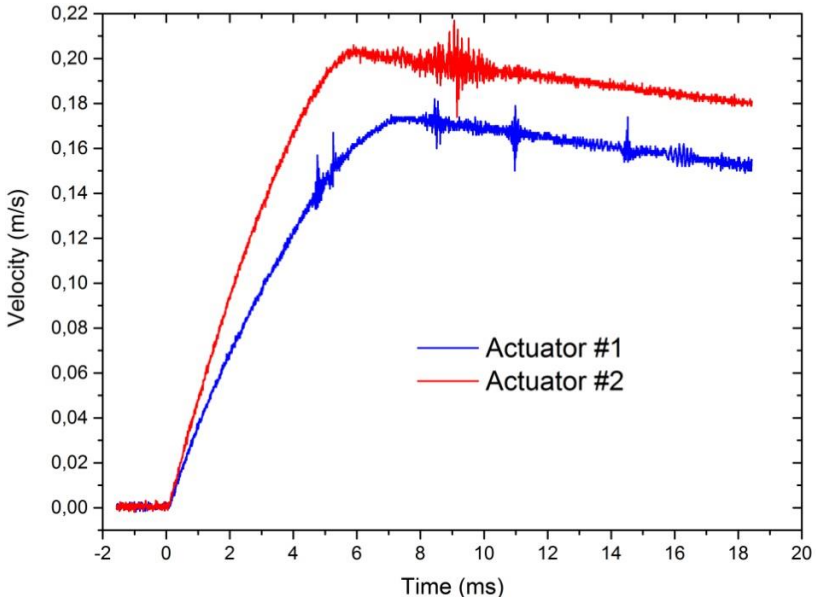

Fig. 39. Velocity *versus* time measured for both actuators (accelerating weight of 102 g).

3.2 MSM effect based haptic device (device and properties)

3.2.1 Physical structure of push-push MSM actuator system

Our device is composed of a "Push-Push" Actuators system which will move an Aluminum 4x4 inches plate. This plate can travel from 0.01 mm to 0.8 mm to "Right-Left". Therefore if someone takes his/her fingertip on the plate, the "Tangentional Skin Displacement" or "Stretch" will happen.

As shown in Fig. 40 two MSM actuators are connected to a Car Stereo Audio Amplifier of 2x35 W, which is powered by a power supply 18 V and has two channels (Ch #1, Ch #2). These two channels are connected to a Digital Analog Converter (DAC). Through a National Instrument (NI) card, which is connected to a PC, the results can be observed by user.

In Fig. 41 the process of providing stroke is illustrated. At (a), the MSM Ni-Mn-Ga active element inside actuator #2, is expanded along its length (horizontally) and generates a force around 1-2 N on plastic stick which pushes the Aluminum plate to left direction around 0.6-0.8 mm. At the same time, the other plastic stick pushes active element inside actuator #1 around 0.6-0.8 mm therefore the active element is contracted vertically. All this process happens in 5 ms. Quite opposite of this process can start from actuator #1 and ends

at actuator #2 as shown in (b).

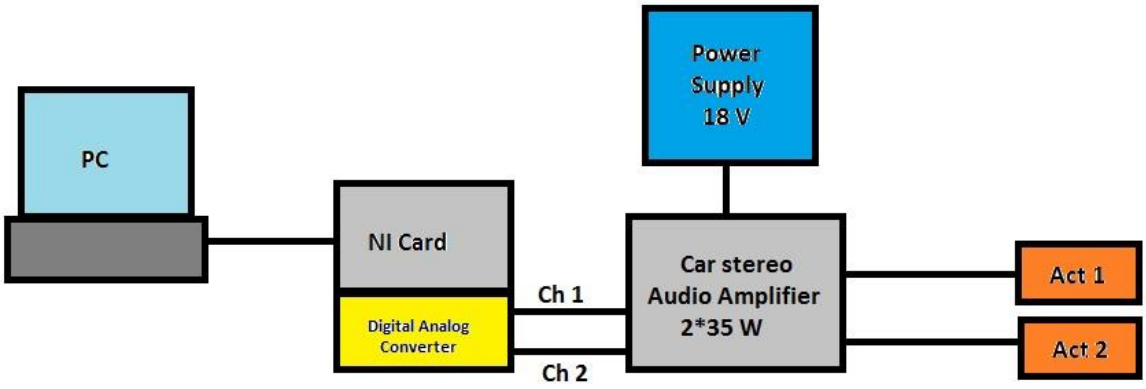

Fig. 40. System structure of push-push design MSM actuators.

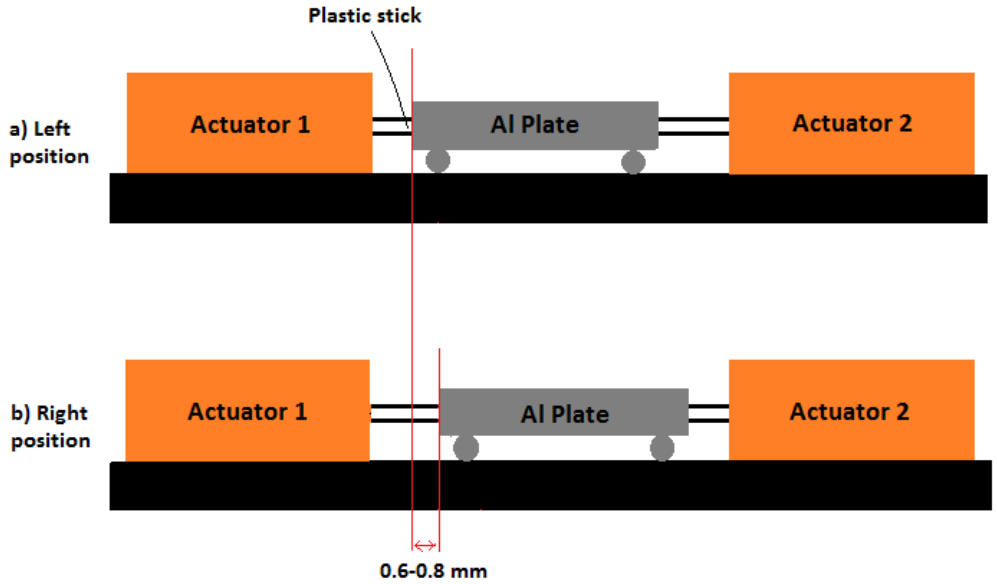

Fig. 41. Process of creation stroke by push-push MSM actuators, (a) actuator #2 create stroke to the left and (b) actuator #1 provide stroke to the right.

3.2.2 System parameters

In this section some parameters of push-push MSM actuator system such as waveforms, frequency, raise time, power consumption, displacement and others are discussed.

As shown in Fig. 42 the device is able to create different types of waveforms such as square, sawtooth and a combination of them. In Fig. 42 (a) at first the Aluminum plate is in rest at left position. Here the energy consumption is 0. Within 5 ms and consuming energy

the plate can go to right position and stay there for an unlimited time t1 without energy consumption. Again within 5 ms plate can come back to left position and stay there for an unlimited time. This process can be repeated with different time t2, t3... (b) Also amplitude of transition from left to right or right to left can be differentiate as shown in figure. It can be from 0 up to maximum 0.8 mm. (c) Other possibility is not having rest at left or right positions therefore within 20 ms 2 journey is possible and by increasing time different Haptic patterns can be generate and transparently be felt by user.

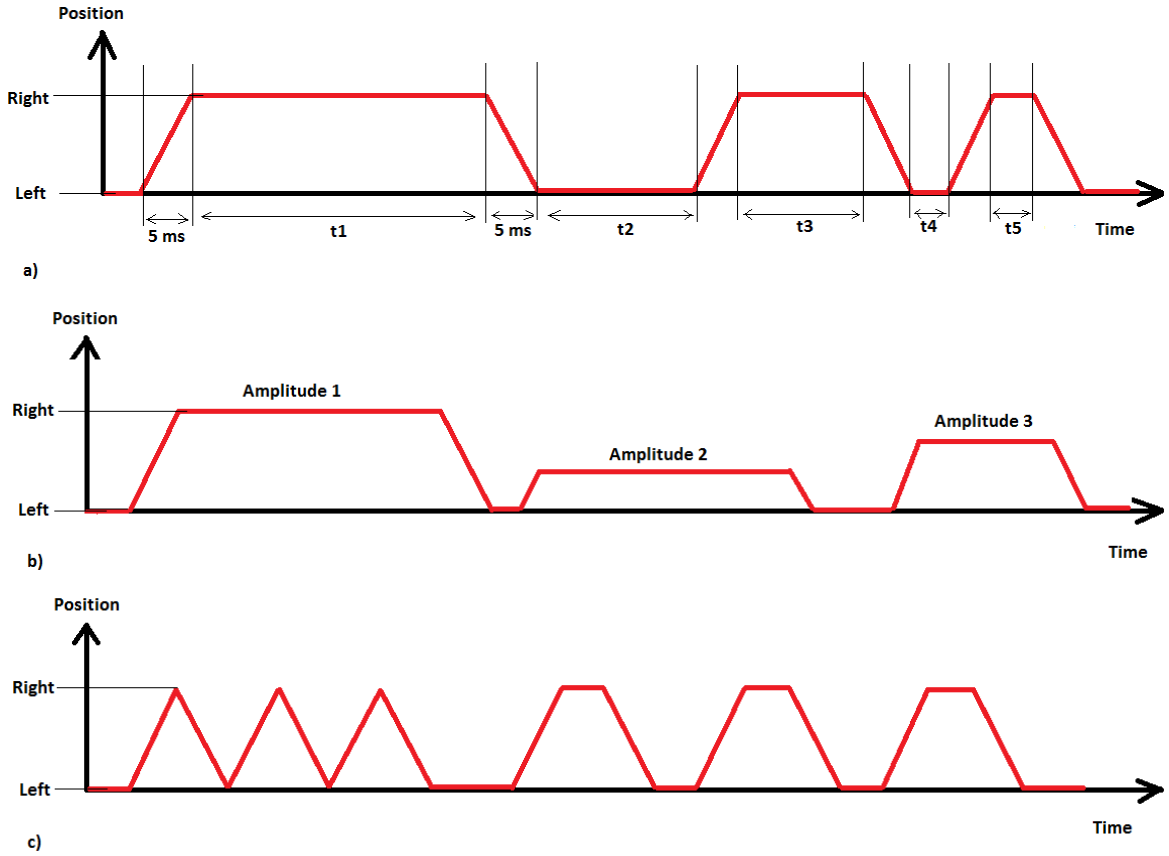

Fig. 42. Different waveforms of device, (a) constant amplitude and various duration, (b) different amplitudes and (c) sawtooth waveforms combined with square waveforms.

In Fig. 43 we demonstrate the graphs of velocity of metal weight in front of the actuator, displacement of weight, the current in which the actuator is driven and the power consumption of our actuators in a fixed time of 100 ms. It is imperative to keep in mind that the frequency in all of mentioned parameters is fixed and ~100 Hz. In all displacement figure it is obvious that the weight starts to move from an unknown place which is

considered as 0. After ~5 ms it reaches to maximum displacement of 0.6-0.88 mm (left or right).

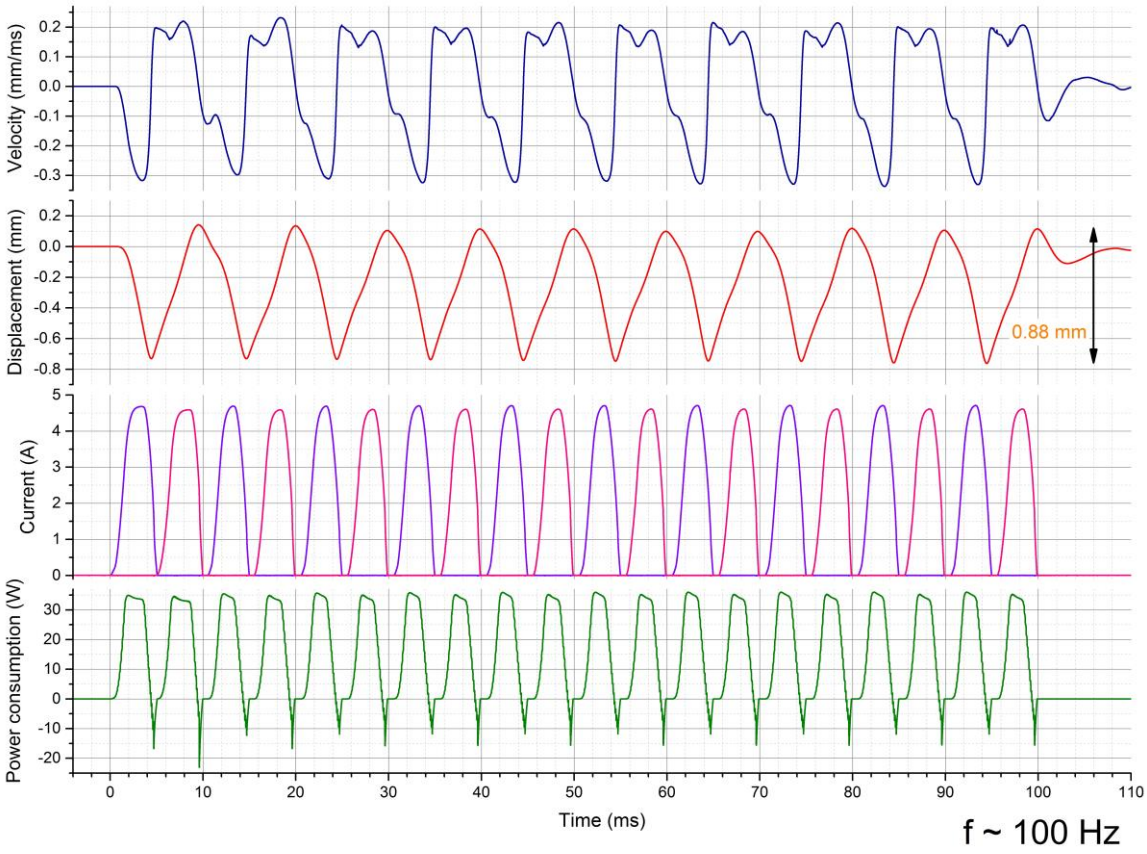

Fig. 43. Velocity, displacement, current and power consumption of MSM actuators.

In the Table 7 we compare the different parameters of various types of actuators with the proposing MSM actuator. One of the most important advantageous of piezoelectric actuators over traditional ones like ERM or LRA is the mechanical time constant. Here MSM actuator can produce the same mechanical time constant as piezoelectric actuators. Also our MSM actuator is able to provide a wide range of frequency from up to 300 Hz which again is far more than that ERM, LRA and the same as Piezos and EAPs that right now are very popular in the market.

3.2.3 Testing of device's haptic feedbacks

3.2.3.1 Experiment of absolute threshold

First of all we prepared an experiment to find out the threshold perception amplitude of the actuator. Since the maximum amplitude is ~0.6-0.8 we were interested to know the

threshold perception.

Table 7. Comparison between different types of actuators in the market.

	ERM	LRA	Piezo	EAP	MSM
Approximate size	11x4.5 mm	10x3.6 mm	3.5x3.5x42 mm	45x38x0.8 mm	1x2.2x20 mm
Power requirement	130-160 mA RMS at 3 V	65-70 mA RMS at 3 V	300 mA RMS at 3 V	Ask vender	5 A at 18 V
Frequency range	90-200 Hz	150-200 Hz	150-300 Hz	90-125 Hz	100-300 Hz
Mechanical time constant	50 ms	30 ms	< 5 ms	< 5 ms	~5-6 ms
Durability	Variable	Very durable	Very durable	Excellent	Durable
Fidelity of sensation	Low	Medium	High	High	High

The environment of experiment is shown in Fig. 44. As you see, the test room is separated to two sides by a thin wall. One side for participant and the other side for examiner. The separation is needed since the participant does not allow to being disturbed by seeing the reactions of examiner. Also he/she must not hear any sound. Therefore the participants have to wear a headphone to hear a pink noise during the examination.

Now that every things are prepared we can test the threshold perception of the actuator. There are 11 different amplitude patterns (0.05, 0.75,...) that each has a duration of 1393 ms. In every patterns we have 21 pulses with the same amplitude but after every 7 pulses we have a pause of 150 ms. To find out the best result we created a random list of 33 patterns which every amplitude have three patterns as shown in Table 8. The results shows that the absolute threshold perception of amplitude is the amplitude 0.2 since for amplitudes 0.2 and more than that each participants could perceive the patterns as 100%.

3.2.3.2 Experiment of 5 different haptic feedbacks

To provide sensation haptic feedbacks we should focus on the haptic parameters as mentioned in second chapter. These parameters are frequency, amplitude, waveform,

spatial location, duration and rhythm.

Table 8. Testing different amplitude to find absolute threshold.

	0.05	0.75	0.1	0.125	0.15	0.175	0.2	0.225	0.25	0.275	0.3
#1	0/3	0/3	0/3	2/3	0/3	3/3	3/3	3/3	3/3	3/3	3/3
#2	0/3	0/3	2/3	2/3	1/3	3/3	3/3	3/3	3/3	3/3	3/3
#3	0/3	0/3	0/3	0/3	1/3	3/3	3/3	3/3	3/3	3/3	3/3
#4	0/3	0/3	0/3	0/3	0/3	1/3	3/3	3/3	3/3	3/3	3/3
%	%0	%0	%16.66	%33.33	%16.66	%91.66	%100	%100	%100	%100	%100

Fig. 44. The environment of test room.

As I mentioned above in all experiments the MSM actuators are driven in the frequency of ~100 Hz. Also the waveforms are in square shape since in sawtooth waveforms the perception is a little bit uncomfortable. This prototype is made to exam the haptic feedbacks on the static participant's fingertip over the surface, therefore the parameter spatial location is automatically not being tested. According to the definition of rhythm, it is a stimulus which has numbers of pulses with some delays between them thus in the

experiment we have 5 rhymes.

Duration and amplitude are parameters which we worked on them carefully. As shown in top part of Fig. 45, there are five patterns that just the amplitude is changing (constant, rise, fall, fall-rise, rise-fall) but the delay between group pulses are constant. In bottom part of Fig. 45 in contrast, the amplitude is constant but the delays between pulses are different. By changing these parameters we could create a wide range of different patterns which most of them were in a high perception by people.

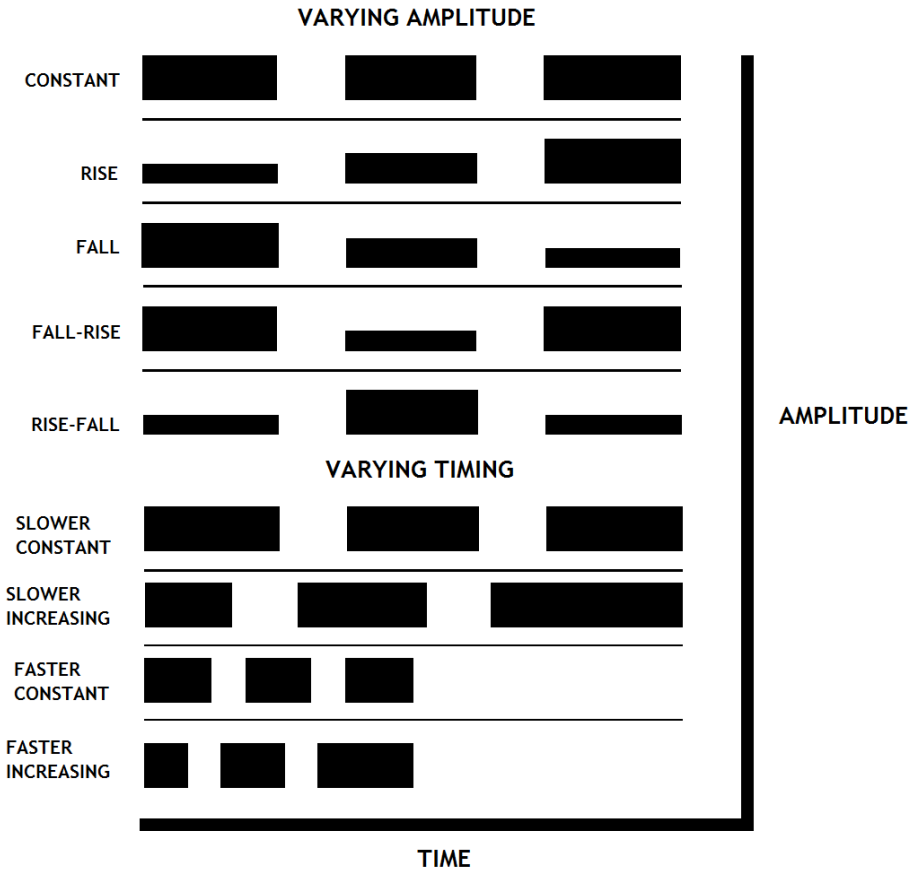

Fig. 45. Creating different haptic patterns by changing the amplitude and duration of pulses.

According to all above information we introduced five final patterns to be tested by participants. Schematic figure of those five patterns as constant, falling (smooth), rising (smooth), falling-rising and rising-falling are demonstrated in below.

For instance the constant pattern is made of 12, Fig. 46, pulses that between every four pulses there is a 150 ms pause. Every pulse is composed of (5-6 ms rise time + 40-41 ms

stay in maximum + 5-6 ms falling time + 40-41 ms stay) therefore the total duration was 1350 ms and of course with maximum amplitude.

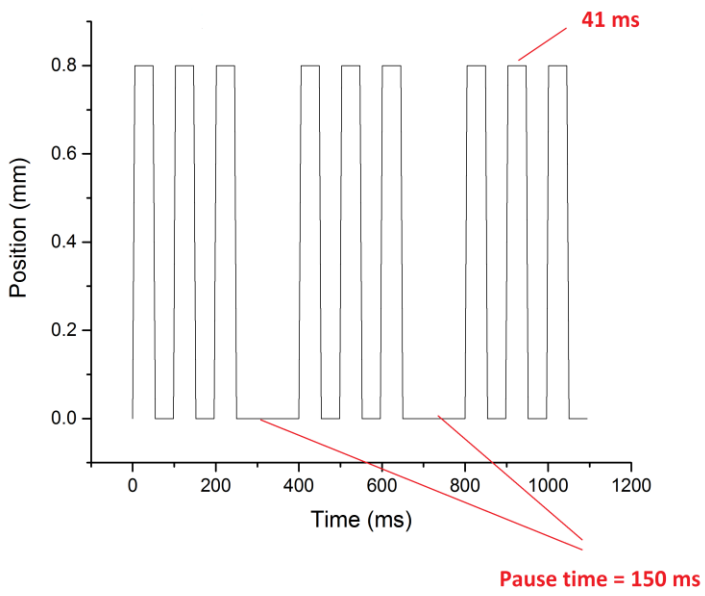

Fig. 46. A sample of constant amplitude pattern with big pauses among pulses.

A schematic view of other four patterns are shown in Fig. 47. In falling pattern we did not use big pause of 150 ms and also the small pause between rising and falling time decreased from 41 ms in constant pattern to 22 ms. Therefore it seems smooth falling meaning the amplitude starts from maximum ~0.8 and slowly decrease to even below absolute threshold which is 0.2 (0.8, 0.75, 0.60,…,0.25, 0.2, 0.15). The same process happens also for smooth rising model when the amplitude starts from below absolute perception and slowly increasing to maximum. Duration of both patterns are 1100 ms.

Rising-falling (Bump) pattern starts from absolute threshold amplitude of 0.2 and after a big delay of 150 ms suddenly increase to maximum and again after passing some pulses it suddenly decrease to absolute threshold amplitude of 0.2. Hole (Falling-rising) model is the same but starts from falling and finishes with rising. Here in this two patterns the duration is 1350 ms.

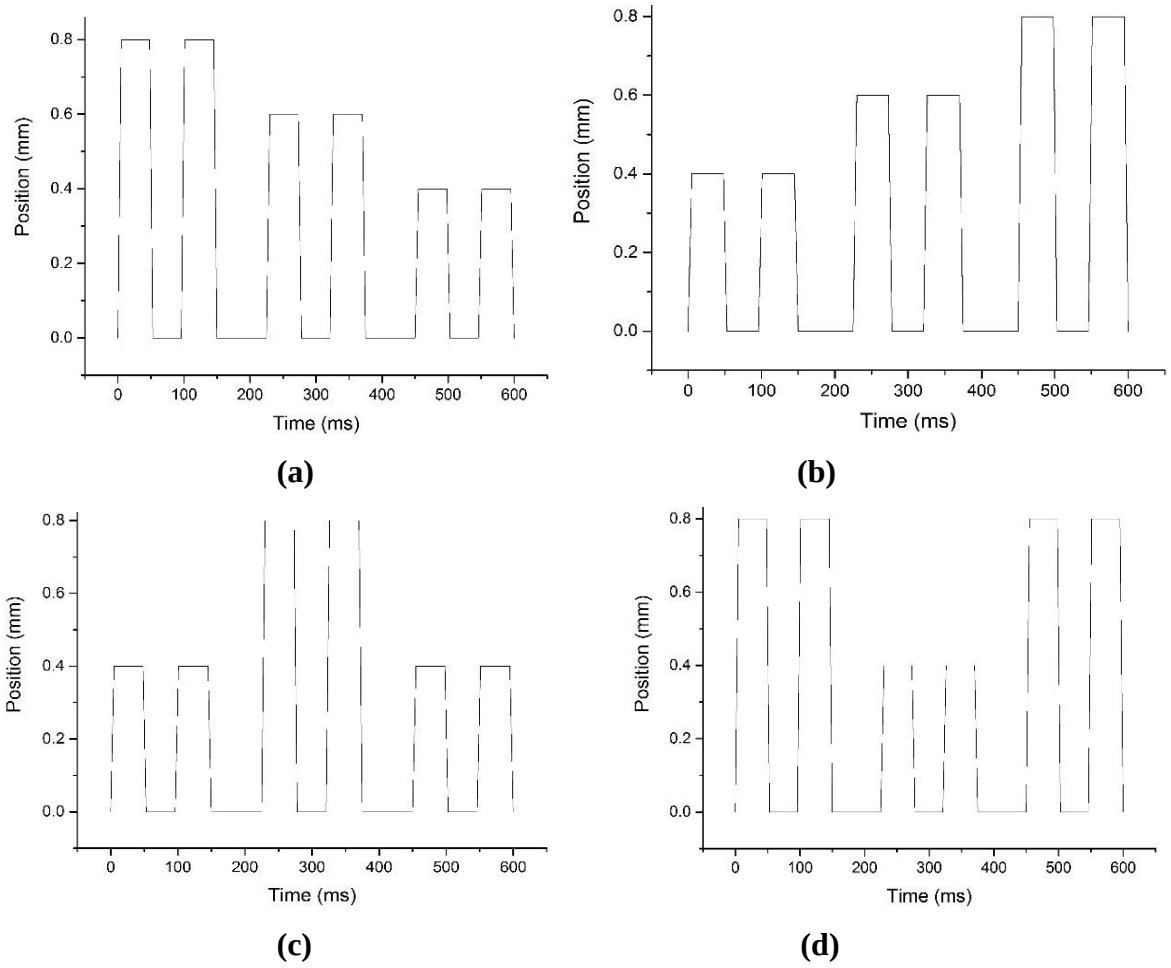

Fig. 47. Four haptic patterns of MSM actuator system which has different amplitudes, (a) falling amplitude, (b) rising amplitude, (c) bump and (d) hole.

For participants to test these five patterns the atmosphere of experiment is the same as before. We invited 8 adults male participants age from (25-60) to take part in our examination. First they were introduced to five patterns by examine all of them before real experiment. They were told that during the test they will have the Fig. 48 in front of themselves to not forget the patterns.

We created 8 lists for each participants. Each of these (constant, falling, rising, hole and bump) had 6 patterns which randomly combined in the list. Therefore each lists had 30 patterns. When examiner from other side of the wall singed, after 10 sec the participant could able to perceive the vibration and tell it loudly enough that the second examiner write it in the study paper.

The final results are shown in table below. Since three was perceived by 100% and the other two are 95% and 85% we can claim that the MSM actuators are able to provide very rich haptic feedbacks.

Fig. 48. Symbolic figures of five patterns that participant watch while he/she is tested.

Table 9. The final results of sensation of five haptic feedbacks.

	Constant	Falling	Rising	Hole	Bump	Not sure
#1	5/6	6/6	6/6	4/6	6/6	
#2	6/6	6/6	6/6	6/6	6/6	
#3	5/6	6/6	6/6	6/6	6/6	
#4	6/6	6/6	6/6	6/6	6/6	
#5	6/6	6/6	6/6	6/6	6/6	
#6	6/6	6/6	6/6	6/6	6/6	
#7	4/6	6/6	6/6	5/5	6/6	
#8	3/6	6/6	6/6	6/6	6/6	
%	85.41%	100%	100%	95.74%	100%	

4 DISCUSSION AND CONCLUSIONS

In this project, firstly we discussed the idea of creation actuation using MSM effect which was invented just two decades before and therefore is a very young and a state of the art phenomenon. Currently used actuators in the market are actuators such as ERM, LRA, piezoelectric, EPA, AMA and others. But mostly people use piezoactuators. Time response of piezoelectric actuators is quite fast but its control and small stroke are its problems.

In our push-push actuator system we produced a stroke in range of millimeter which is significant compare to piezoelectric actuators. Also the time response is quite fast around 5 ms that is the same range of piezo actuators.

Secondly we mentioned a very complete list of vibrotactile devices that uses actuators to produce haptic feedbacks on skin.

In third part we introduced our push-push actuator haptic system to produce haptic feedbacks on participant's fingertip. We held two experiments. In experiment 1 we found out the absolute threshold which was ~0.2 in amplitude. In the second experiment we tested five different haptic patterns that were perceived by good results. One was perceived by 85%, one by 95% and three were sensed by 100%.

There are some possibilities for future to run the device and seems the results will be more significant than current ones.

We can change the frequency in the range of 0-300 Hz. In this project we just have used the frequency 100 Hz.

Also we can use the idea of LateralPad and attach piezos under the surface to produce a vertical vibration and therefore squeeze film air effect. Since horizontal vibration will be provided by MSM actuator which is more controllable than piezos in Lateral Pad, the results will be more reliable.

5 SUMMARY

The aim of this project is to create rich haptic feedbacks using a new type of MSM actuators. We create a push-push actuator system which vibrate a surface between themselves and deliver haptic vibrations on the fingertip. For this reason we hold two experiments for testing the absolute threshold and five different haptic feedbacks.

In the first experiment we tested the device by four participants and found that the absolute amplitude threshold is ~0.2. This amplitude and amplitudes more than that are perceived with 100%.

In the second experiment we tested five different haptic feedbacks such as constant amplitude, falling amplitude, rising amplitude, Bump and Hole. Eight male participants in the range of 26-60 years are tested.

Perception of constant amplitude is 85.4%. For the falling amplitude the sensation is 100%. This perception is 100%, 95.4% and 100% for rising amplitude, Hole and Bump respectively.

All experiments are held in frequency of 100 Hz, duration range of 1.2-1.5 sec and square waveforms.

REFERENCES

1. Yang GH, Kyung KU, Srinivasan MA, Kwon DS. Quantitative tactile display device with pin-array type tactile feedback and thermal feedback. InRobotics and Automation, 2006. ICRA 2006. Proceedings 2006 IEEE International Conference on 2006 May 15 (pp. 3917-3922). IEEE.
2. Pasquero J, Hayward V. STReSS: A practical tactile display system with one millimeter spatial resolution and 700 Hz refresh rate. InProc. Eurohaptics 2003 Jul (Vol. 2003, pp. 94-110).
3. Velázquez R, Pissaloux EE, Wiertlewski M. A compact tactile display for the blind with shape memory alloys. InRobotics and Automation, 2006. ICRA 2006. Proceedings 2006 IEEE International Conference on 2006 May 15 (pp. 3905-3910). IEEE.
4. Levesque V, Oram L, MacLean K, Cockburn A, Marchuk ND, Johnson D, Colgate JE, Peshkin MA. Enhancing physicality in touch interaction with programmable friction. InProceedings of the SIGCHI Conference on Human Factors in Computing Systems 2011 May 7 (pp. 2481-2490). ACM.
5. Kotani H, Takasaki M, Mizuno T. Surface acoustic wave tactile display using a large size glass transducer. InMechatronics and Automation, 2007. ICMA 2007. International Conference on 2007 Aug 5 (pp. 198-203). IEEE.
6. Bau O, Poupyrev I, Israr A, Harrison C. TeslaTouch: electrovibration for touch surfaces. InProceedings of the 23nd annual ACM symposium on User interface software and technology 2010 Oct 3 (pp. 283-292). ACM.
7. Dai X, Colgate JE, Peshkin MA. LateralPaD: A surface-haptic device that produces lateral forces on a bare finger. InHaptics Symposium (HAPTICS), 2012 IEEE 2012 Mar 4 (pp. 7-14). IEEE.
8. Hoggan E, Brewster SA, Johnston J. Investigating the effectiveness of tactile feedback for mobile touchscreens. InProceedings of the SIGCHI conference on Human factors in computing systems 2008 Apr 6 (pp. 1573-1582). ACM.
9. Yatani K, Truong KN. SemFeel: a user interface with semantic tactile feedback for mobile touch-screen devices. InProceedings of the 22nd annual ACM symposium on User interface software and technology 2009 Oct 4 (pp. 111-120). ACM.

10. Fukumoto M, Sugimura T. Active click: tactile feedback for touch panels. InCHI'01 Extended Abstracts on Human Factors in Computing Systems 2001 Mar 31 (pp. 121-122). ACM.
11. Brewster S, Brown LM. Tactons: structured tactile messages for non-visual information display. InProceedings of the fifth conference on Australasian user interface-Volume 28 2004 Jan 1 (pp. 15-23). Australian Computer Society, Inc..
12. Yang TH, Kim SY, Kim CH, Kwon DS, Book WJ. Development of a miniature pin-array tactile module using elastic and electromagnetic force for mobile devices. InEuroHaptics conference, 2009 and Symposium on Haptic Interfaces for Virtual Environment and Teleoperator Systems. World Haptics 2009. Third Joint 2009 Mar 18 (pp. 13-17). IEEE.
13. Poupyrev I, Maruyama S. Tactile interfaces for small touch screens. InProceedings of the 16th annual ACM symposium on User interface software and technology 2003 Nov 2 (pp. 217-220). ACM.
14. Poupyrev I, Maruyama S, Rekimoto J. Ambient touch: designing tactile interfaces for handheld devices. InProceedings of the 15th annual ACM symposium on User interface software and technology 2002 Oct 27 (pp. 51-60). ACM.
15. Ullakko K. Magnetically controlled shape memory alloys: a new class of actuator materials. Journal of materials Engineering and Performance. 1996 Jun 1;5(3):405.
16. Yeduru SR. Development of Microactuators Based on the Magnetic Shape Memory Effect. KIT Scientific Publishing; 2013 Dec 10.''doctoral thesis''
17. Otsuka K, Wayman CM, editors. Shape memory materials. Cambridge university press; 1999 Oct 7.
18. Chopra I, Sirohi J. Smart structures theory. Cambridge University Press; 2013 Dec 30.
19. Buehler WJ, Gilfrich JV, Wiley RC. Effect of low-temperature phase changes on the mechanical properties of alloys near composition TiNi. Journal of applied physics. 1963 May;34(5):1475-7.
20. Krulevitch P, Lee AP, Ramsey PB, Trevino JC, Hamilton J, Northrup MA. Thin film shape memory alloy microactuators. Journal of Microelectromechanical Systems. 1996 Dec;5(4):270-82.

21. Murray SJ, Marioni MI, Allen SM, O'handley RC, Lograsso TA. 6% magnetic-field-induced strain by twin-boundary motion in ferromagnetic Ni–Mn–Ga. Applied Physics Letters. 2000 Aug 7;77(6):886-8.
22. Sozinov A, Likhachev AA, Lanska N, Ullakko K. Giant magnetic-field-induced strain in NiMnGa seven-layered martensitic phase. Applied Physics Letters. 2002 Mar 11;80(10):1746-8.
23. Dunand DC, Müllner P. Size Effects on Magnetic Actuation in Ni-Mn-Ga Shape-Memory Alloys. Advanced Materials. 2011 Jan 11;23(2):216-32.
24. Schiepp T. A Simulation Method for Design and Development of Magnetic Shape Memory Actuators (Doctoral dissertation, University of Gloucestershire).
25. Karaman I, Basaran B, Karaca HE, Karsilayan AI, Chumlyakov YI. Energy harvesting using martensite variant reorientation mechanism in a NiMnGa magnetic shape memory alloy. Applied Physics Letters. 2007 Apr 23;90(17):172505.
26. https://commons.wikimedia.org/wiki/File:MSM_principle_Schnetzler2016.png.
27. Straka L. Magnetic and magneto-mechanical properties of Ni-Mn-Ga magnetic shape memory alloys. ''doctoral thesis''
28. Smith AR. New methods for controlling twin configurations and characterizing twin boundaries in 5M Ni-Mn-Ga for the development of applications. Acta Universitatis Lappeenrantaensis. 2015 Jun 10.''doctoral thesis''
29. http://www.geocities.jp/ohba_lab_ob_page/structure2.html
30. https://www.boundless.com/biology/textbooks/boundless-biology-textbook/sensory-systems-36/somatosensation-206/somatosensory-receptors-778-12012/
31. http://doctorlib.info/physiology/review/11.html
32. Yatani K. *{Spatial Tactile Feedback Support for Mobile Touch-screen Devices* (Doctoral dissertation).
33. Rantala J. Spatial Touch in Presenting Information with Mobile Devices.''doctoral thesis''
34. Yatani K, Truong KN. SemFeel: a user interface with semantic tactile feedback for mobile touch-screen devices. InProceedings of the 22nd annual ACM symposium on User interface software and technology 2009 Oct 4 (pp. 111-120). ACM.

35. Kyung KU, Lee J, Park JS. Pen-like haptic interface and its application on touch screen. InRobot and Human interactive Communication, 2007. RO-MAN 2007. The 16th IEEE International Symposium on 2007 Aug 26 (pp. 9-13). IEEE.
36. Fukumoto M, Sugimura T. Active click: tactile feedback for touch panels. InCHI'01 Extended Abstracts on Human Factors in Computing Systems 2001 Mar 31 (pp. 121-122). ACM.
37. Brewster S, Brown LM. Tactons: structured tactile messages for non-visual information display. InProceedings of the fifth conference on Australasian user interface-Volume 28 2004 Jan 1 (pp. 15-23). Australian Computer Society, Inc..
38. Brown LM, Brewster SA, Purchase HC. Multidimensional tactons for non-visual information presentation in mobile devices. InProceedings of the 8th conference on Human-computer interaction with mobile devices and services 2006 Sep 12 (pp. 231-238). ACM.
39. Shin H, Lim JM, Lee JU, Kyung KU, Lee G. Tactile feedback for button GUI on touch devices. InCHI'12 Extended Abstracts on Human Factors in Computing Systems 2012 May 5 (pp. 2633-2636). ACM.
40. Harrison C, Hudson SE. Providing dynamically changeable physical buttons on a visual display. InProceedings of the SIGCHI Conference on Human Factors in Computing Systems 2009 Apr 4 (pp. 299-308). ACM.
41. Jansen Y, Karrer T, Borchers J. MudPad: tactile feedback and haptic texture overlay for touch surfaces. InACM International Conference on Interactive Tabletops and Surfaces 2010 Nov 7 (pp. 11-14). ACM.
42. Carter T, Seah SA, Long B, Drinkwater B, Subramanian S. UltraHaptics: multi-point mid-air haptic feedback for touch surfaces. InProceedings of the 26th annual ACM symposium on User interface software and technology 2013 Oct 8 (pp. 505-514). ACM.
43. Altinsoy ME, Merchel S. Electrotactile feedback for handheld devices with touch screen and simulation of roughness. IEEE Transactions on Haptics. 2012 Jan;5(1):6-13.
44. Watanabe T, Fukui S. A method for controlling tactile sensation of surface roughness using ultrasonic vibration. InRobotics and Automation, 1995.

Proceedings., 1995 IEEE International Conference on 1995 May 21 (Vol. 1, pp. 1134-1139). IEEE.

45. Wang Q, Ren X, Sun X. Enhancing Pen-based Interaction using Electrovibration and Vibration Haptic Feedback. InProceedings of the 2017 CHI Conference on Human Factors in Computing Systems 2017 May 2 (pp. 3746-3750). ACM.
46. Chubb EC, Colgate JE, Peshkin MA. ShiverPad: A device capable of controlling shear force on a bare finger. InEuroHaptics conference, 2009 and Symposium on Haptic Interfaces for Virtual Environment and Teleoperator Systems. World Haptics 2009. Third Joint 2009 Mar 18 (pp. 18-23). IEEE.
47. Winfield L, Glassmire J, Colgate JE, Peshkin M. T-pad: Tactile pattern display through variable friction reduction. InEuroHaptics Conference, 2007 and Symposium on Haptic Interfaces for Virtual Environment and Teleoperator Systems. World Haptics 2007. Second Joint 2007 Mar 22 (pp. 421-426). IEEE.
48. Chubb EC, Colgate JE, Peshkin MA. Shiverpad: A glass haptic surface that produces shear force on a bare finger. IEEE Transactions on Haptics. 2010 Jul;3(3):189-98.
49. Dai X, Colgate JE, Peshkin MA. LateralPaD: A surface-haptic device that produces lateral forces on a bare finger. InHaptics Symposium (HAPTICS), 2012 IEEE 2012 Mar 4 (pp. 7-14). IEEE.